

LAMONT-DOHERTY GEOLOGICAL OBSERVATORY
OF COLUMBIA UNIVERSITY

PALISADES, NEW YORK

COMPOSITE DRILL STEM OF EPOXY FIBER GLASS REINFORCED WITH BORON
FILAMENTS AND A RETRIEVABLE CORE LINER/SAMPLE RETURN CONTAINER
FOR THE APOLLO LUNAR SURFACE DRILL

by
Marcus G. Langseth, Jr.
Harry A. Gibbon
Richard S. Perry



Technical Report No. 2 CU-2-70
Contract NAS 9-6037

Sponsored by the National Aeronautics and Space Administration

August 1970

| | | |
|-------------------|-------------------------------|------------|
| FACILITY FORM 602 | N70-40770 | |
| | (ACCESSION NUMBER) | (THRU) |
| | 80 | 1 |
| | (PAGES) | (CODE) |
| | CR-108640 | 15 |
| | (NASA CR OR TMX OR AD NUMBER) | (CATEGORY) |

CR-108640

LAMONT-DOHERTY GEOLOGICAL OBSERVATORY OF COLUMBIA UNIVERSITY

PALISADES, NEW YORK 10964

COMPOSITE DRILL STEM OF EPOXY FIBER GLASS
REINFORCED WITH BORON FILAMENTS
AND A RETRIEVABLE CORE LINER/SAMPLE RETURN CONTAINER
FOR THE APOLLO LUNAR SURFACE DRILL

by

Marcus G. Langseth, Jr.
Harry A. Gibbon
Richard S. Perry

Technical Report No. 2 Cu-2-70
Contract NAS 9-6037

Sponsored by the National Aeronautics and Space Administration

August 1970

Reproduction of this document in whole or in part is permitted for any purpose of the U.S. Government.

LIST OF ILLUSTRATIONS

| | Page |
|---|------|
| FIGURE 1. An assembly drawing of the boron reinforced fiber glass drill stem, bit adapter section and bit | 8 |
| FIGURE 2. Detail of boron reinforced drill stem showing structure | 9 |
| Figure 3. Plot of drilling rate versus bit kerf area based on tests at L-DGO | 14 |
| FIGURE 4. The female taper joint showing details of layering of glass and boron filaments | 17 |
| FIGURE 5. Plot of measured bit temperatures versus drilling time in dense basalt | 18 |
| FIGURE 6. Photograph of early development model solid bit | 20 |
| FIGURE 7. Photograph of final solid-face drill bit | 20 |
| FIGURE 8. Photograph of a complete core retrieval system, prototype model | 23 |
| FIGURE 9. Close-up photograph of the wiper seal at the end of the core liner | 24 |
| FIGURE 10. Close-up of the core catcher | 24 |
| FIGURE 11. The disassembled components of a development core lock | 26 |
| FIGURE 12. The final core lock design | 26 |
| FIGURE 13. An assembly drawing of the core lock mechanism | 27 |
| FIGURE 14. Close-up photograph of core lock/core liner attachment mechanism | 28 |
| FIGURE 15. Photograph of locking joint used in the emplacement/retrieval tool stem sections | 28 |
| FIGURE 16. Three views of the torque-limiting wrench handle | 30 |

TABLE OF CONTENTS

| | |
|---|----|
| SUMMARY | 1 |
| BACKGROUND | 2 |
| DESIGN REQUIREMENTS | 5 |
| SUBCONTRACTING ARRANGEMENTS | 7 |
| PROGRAM DEVELOPMENTS AND TEST RESULTS | 7 |
| A. Boron Filament Reinforced Fiber Glass Drill Stem | 7 |
| 1. Drill Stem Body | 7 |
| 2. Taper Joint | 15 |
| 3. Bit Adapter Section | 16 |
| B. Solid-Face Bit | 19 |
| C. Core Retrieval System | 21 |
| ITEMS DELIVERED UNDER THIS PROGRAM | 31 |
| RECOMMENDATIONS FOR FUTURE WORK | 31 |

APPENDIXES

- A - Application of a Glass/Boron Composite to the ALSD bit Extension
- B - Thermal Conductivity Measurements of Boron-Reinforced Fiber Glass Tube
- C - Preliminary Report - Drill Tests During January (1969)
- D - Report of Tests to Measure the Rise of Bit Temperatures During the Drilling of Dense Basalt

SUMMARY

This report describes the development of a drill stem to be used with the Apollo Lunar Surface Drill to drill holes in the moon's surface to emplace the lunar heat flow experiment, and the subsequent development of a prototype model of a core retrieval system that does not require the removal of the drill stem from the lunar subsurface.

The objectives of the development program were: (a) to reduce the number of tasks, eliminate excessive physical exertion, and reduce the time required to drill two 3-meter heat flow holes in the lunar surface and (b) to increase the quality and quantity of the lunar subsurface soil samples taken from the boreholes.

The program resulted in the development of prototype models of a drill stem made of epoxy fiberglass, reinforced with axially aligned crystalline boron fibers. This stem is compatible with the existing Apollo Lunar Surface Drill powerhead and replaces the titanium drill stem and fiberglass casing initially designed for emplacing the heat flow experiment probes.

The mechanical properties of the composite stem developed under this program (a Young's Modulus of approximately 12 million PSI and high torsion strength) provide a drilling performance nearly equal to that of the titanium drill stem. The thermal conductance of the epoxy-boron stem is approximately $0.01 \text{ watt-cm/}^{\circ}\text{C}$ which is low enough to permit accurate temperature gradient and the conductivity determinations to be made in the lunar soil through the walls of the drill stem.

A solid-face drill bit, 1.125" in diameter, was developed to be used with the boron filament stem. Unlike the original coring bit, this bit removes all material in a 1.125" hole. After drilling the borehole to the required depth with the composite drill stem and solid-face bit, the temperature-sensing probes of the HFE can be directly inserted into the hollow

stem. This eliminates the tasks of retracting the titanium stem and drilling down a separate fiber glass casing required with the original ALS design.

The prototype models described above have been successfully developed into flight hardware by the Martin Marietta Corporation of Denver, Colorado and are now incorporated into the Apollo Lunar Surface Drill design.

In addition, a lunar core sampling system was developed and a prototype fabricated. This system would permit the astronaut to remove core samples from the borehole without retracting the drill stem. The core is collected in thin-walled core liners that are inserted and locked into the lower part of the drill stem. The same liners can be used as sample return containers. This coring system has been successfully tested in uncohesive aggregates of rock powder similar to those thought to compose the lunar surface layer. This system can obtain a more representative sample of the drilled material than the titanium drill stem.

The development work was carried out at the Lamont-Doherty Geological Observatory of Columbia University with assistance from the Martin Marietta Corporation, Arthur D. Little Co., Inc., Chicago-Latrobe, and the AVCO Corporation.

BACKGROUND

The Heat Flow Experiment (HFE) is one of several experiments in the ALSEP program that will be emplaced on the lunar surface during a lunar landing mission. The HFE is designed to measure the heat budget in the shallow subsurface of the moon for a period of one year. This measurement will be achieved by making very precise measurements of temperature difference in the lunar soil together with measurements of the thermal conductivity of the moon's subsurface material. The principal objective is to determine the net loss of heat from the deep interior.

One of the problems in making this type of measurement is how to eliminate the large diurnal surface temperature variation ($\sim 350^{\circ}\text{C}$) induced by the sun. These variations decrease rapidly with depth in the poorly conducting lunar surface layer. If the temperature sensors are 1.5 or more meters below the surface, they would detect variations of only a fraction of a degree and can be subtracted from the steady components we wish to measure. Thus, by burying the heat flow probe 1.5 or more meters we can greatly improve the accuracy of the heat flow determination.

The Apollo Lunar Surface Drill: The ALSD is a system capable of drilling and casing two 3-meter holes with a nominal ID of 0.875" in the lunar soil in which the heat flow probes are buried. The drill system originally delivered to MSC by Martin Marietta consisted of a battery-operated, rotary-percussive power head, 8 sections of titanium drill stem, a coring bit, twelve sections of epoxy fiber glass borehole casing, and auxiliary equipment that included a foot treadle, a storage rack, and a wrench.

The procedure to emplace the first of the two heat flow probes in the lunar surface using the original ALSD is to: (1) drill a ten-foot hole using eight sections of titanium drill stem, (2) retract the drill stem from the hole and empty the core material on the surface, (3) reenter the hole with the fiber glass casing, and (4) insert the first heat-flow probe. To emplace the second probe: (5) drill a ten-foot hole with the titanium stem, (6) retract the drill stem, (7) disconnect each section of stem containing core material and store in hand tool carrier, (8) reenter the hole with the fiber glass casing, and (9) insert the second heat-flow probe.

Many of the tasks can be avoided by using a drill stem that does not have to be retracted from the lunar subsurface. Such a drill stem must have a low thermal conductance, so as not to degrade the heat-flow experiment performance, yet have an axial modulus high enough to effectively transmit the percussive energy of the power head to the bit. To utilize a low conductance drill stem that can be left in the lunar subsurface it is, of course, necessary to develop either a solid-face bit that does not allow material to enter the drill stem, or, if a coring bit is used, to develop a core retrieving system that can remove material from inside the stem.

The approach that seemed most feasible was to replace the titanium drill stem with a stem made of composite material. An epoxy resin was chosen for the matrix of the stem tube because of its low thermal conductivity. The epoxy is strengthened by glass fibers wound circumferentially in the tube walls. The axial stiffness is increased by an order of magnitude by including filaments of crystalline boron (Young's modulus 60×10^6 PSI), aligned with the tube axis.

From the start of the program we hoped to develop a solid-face bit by a modification of the existing ALSD coring bit designed by Martin Marietta and Chicago-Latrobe, thus benefiting from the experience and testing that went into that bit development. Our approach, which proved successful, was to insert a central cutter inside the annulus of cutters of the core bit. When drilling solid rock, the core bit leaves a small cylinder of material standing above the cutting face, this cylinder is broken up by the carbide central cutter.

An alternative to the solid-face bit is to remove the core material from inside the boron drill stem. Because of the great scientific value

of the subsurface core samples, a system that could retrieve the sample would be worth the extra astronaut effort required. To this end we began development of a "core retrieval system." We decided to utilize a system similar to that used in standard drilling techniques. The basic feature of the system is a thin-walled core liner that is locked in the bottom section of the drill stem. These core liners would be inserted and locked in place. After drilling into the lunar subsurface the length of the core liner, it is locked in place and removed by the astronaut. For emplacement and retrieval of the liners a special tool would have to be designed. This liner serves as a core sample container on the return flight.

DESIGN REQUIREMENTS

A. Boron Filament Reinforced Fiber Glass Drill Stem:

1. Stem body: The stem body should have an axial modulus of elasticity sufficiently high so that its drilling rate in dense basalt is comparable to that of the titanium stem. (Young's Modulus of titanium is estimated at about 16×10^6 PSI.)
2. Interstem joints: Because of limited storage space and astronaut handling requirements, the stem is broken down into sections about 22" long. This joint must be rejoined on the surface and must be designed to transmit the percussive energy with little or no attenuation and also transmit the torque from the power head (maximum 30 ft-lbs).
3. Thermal conductance: The conductivity of the composite boron stem should be less than 0.01 watts/cm⁰C in the axial direction.
4. Flutes: Helical flutes are added to the outside of the bore stem to transport cuttings from the drill face to the surface. These flutes must have sufficient wear resistance to maintain their function after drilling up to four minutes in solid rock.

5. Dimensions: If possible the dimensions of the drill stem should be similar to those of the fiber glass casing used on the existing ALSD.

B. Solid-Face Drill Bit:

1. Drill rate: To meet performance requirements the solid-face bit must drill at nearly the same rate as the ALSD core bit. Typical rates are 1 to 2 inches/minute in dense basalt, 4 to 7 inches/minute in vesicular basalt with a 40% void ratio.

2. Thermal considerations: The efficiency of the bit should be high enough to preclude damage to the epoxy resin in the stem due to high temperatures (i.e. $<300^{\circ}\text{F}$). Some means should be provided to thermally isolate the bit from the stem if high temperatures cannot be avoided.

3. Interchangeability: The solid-face bits should be interchangeable between stem sets and with coring bits.

C. Core Retrieval System:

1. Subsurface sampling: The core system should be designed to obtain the maximum sample with the minimum of physical damage to the sample.

2. Operability: The system should be easily operable by a space-suited subject.

3. Core sample return container: The core liners should also serve as a return container storable in the sample return container. (Storage in the SRC is limited to objects that are less than 16.75" in length and are composed of non-organic materials.)

4. Core retention: The liners must retain the core sample when it is retracted from the stem and while being handled by the astronaut.

5. Compatibility: The core retrieval system should be compatible with the boron stem and the ALSD power head.

6. Storage: The system should be designed so that together with the remainder of the ALSD drill system it can be packaged within the existing ALSD volume envelope.

SUBCONTRACTING ARRANGEMENTS

The AVCO Space Systems Division, under a subcontract from L-DGO, was initially chosen to perform the design and development of the composite drill stem. The work was done under the guidance of L-DGO. The subcontract with AVCO consisted to two tasks:

Task I: To conduct a design and manufacturing feasibility study.

Task II: Fabrication of prototype sets of drill stem.

After completing Task I, the subcontract was terminated.

Phase II was completed under a separate subcontract with Arthur D. Little, Inc. This work was also done under the supervision and direction of Lamont-Doherty Geological Observatory.

The development solid-face bits were purchased by L-DGO from Chicago-Latrobe, Inc., based on L-DGO drawings.

PROGRAM DEVELOPMENTS AND TEST RESULTS

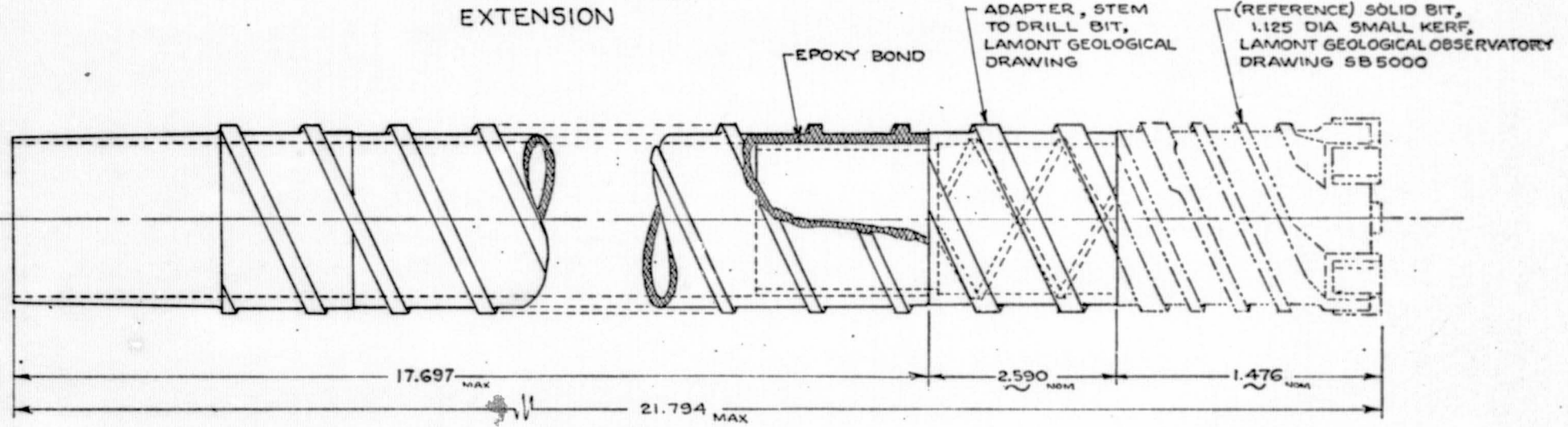
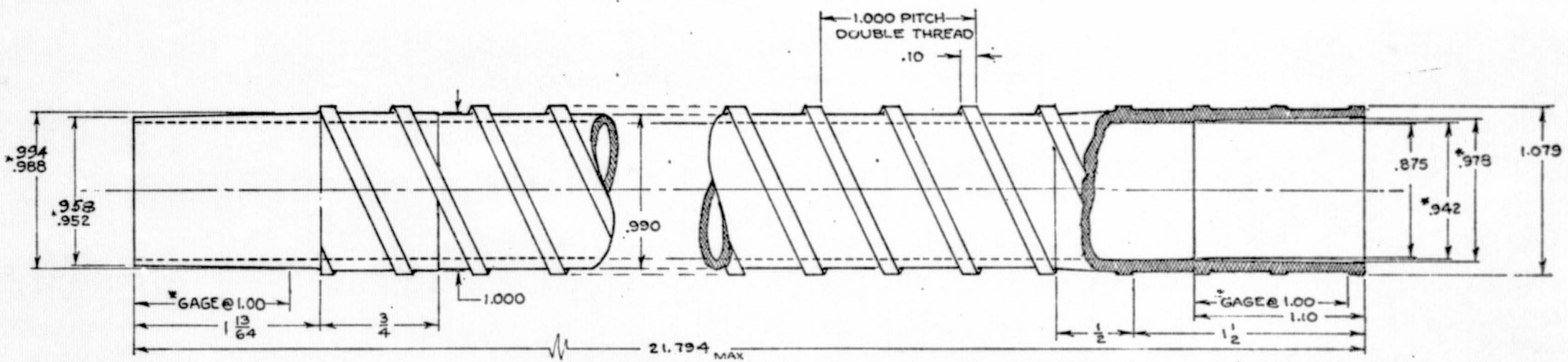
A. Boron Filament Reinforced Fiber Glass Drill Stem:

1. Drill Stem Body: The boron drill stem developed under this program is shown in Figure 1.

(a) Design: The tubular body of the drill stem has a sandwich construction (the details of which are shown in Figure 2). Innermost are two layers of epoxy fiber glass, with the glass filaments, helically wound

This drawing is not to be used for making reproductions thereof, or for making any apparatus based thereon, without first obtaining written authorization of Arthur D. Little, Inc.

| REVISIONS | | | | |
|-----------|-----|--|---------|----------|
| ZONE | LTR | DESCRIPTION | DATE | APPROVED |
| | A | DELETED .028 DIM. GAP BETWEEN ADAPTER STEM AND SOLID BIT, 17.697 DIM. WAS 19.169 & 2.590 DIM WAS 1.090 | 4-22-69 | |



- NOTES
1. GAGING DIMENSIONS ARE MARKED *
 2. DIMENSIONS OF STEM ARE IDENTICAL TO THOSE OF EXTENSION EXCEPT FOR LENGTH AND OMISSION OF FEMALE (TAPERED SOCKET) END.
 3. TAPER IS .036/INCH (REFERENCE).

| ITEM NO. | QTY REQ | PART OR IDENTIFYING NO. | NOMENCLATURE OR DESCRIPTION | MATERIAL |
|---------------|---------|-------------------------|-----------------------------|----------|
| LIST OF PARTS | | | | |

| | | | | | |
|--|---|-------------------------------------|--|---|--|
| UNLESS OTHERWISE SPECIFIED | | ISSUE DATE: | | Arthur D. Little, Inc. CAMBRIDGE, MASSACHUSETTS 02140 | |
| DIMENSIONS ARE IN INCHES | | DRAWN <i>J. W. Sullivan</i> 10APR69 | | | |
| TOLERANCES: | | CHECKED | | LUNAR DRILL STRING | |
| DECIMAL .XX = ± .XXX = ± | FRACTIONAL $\frac{1}{2}$ ANGULAR ± | APPROVED | | | |
| FINISHED SURFACES BREAK SHARP CORNERS | | RMS R | | SIZE C CODE IDENT NO. 71197-10 REVISION A | |
| DO NOT SCALE THIS DRAWING | | MATERIAL | | | |
| NEXT APPY | | USED ON | | SCALE 2:1 SHEET | |
| APPLICATION | | CARE | | | |

FIG. 1

C 71197-10 A

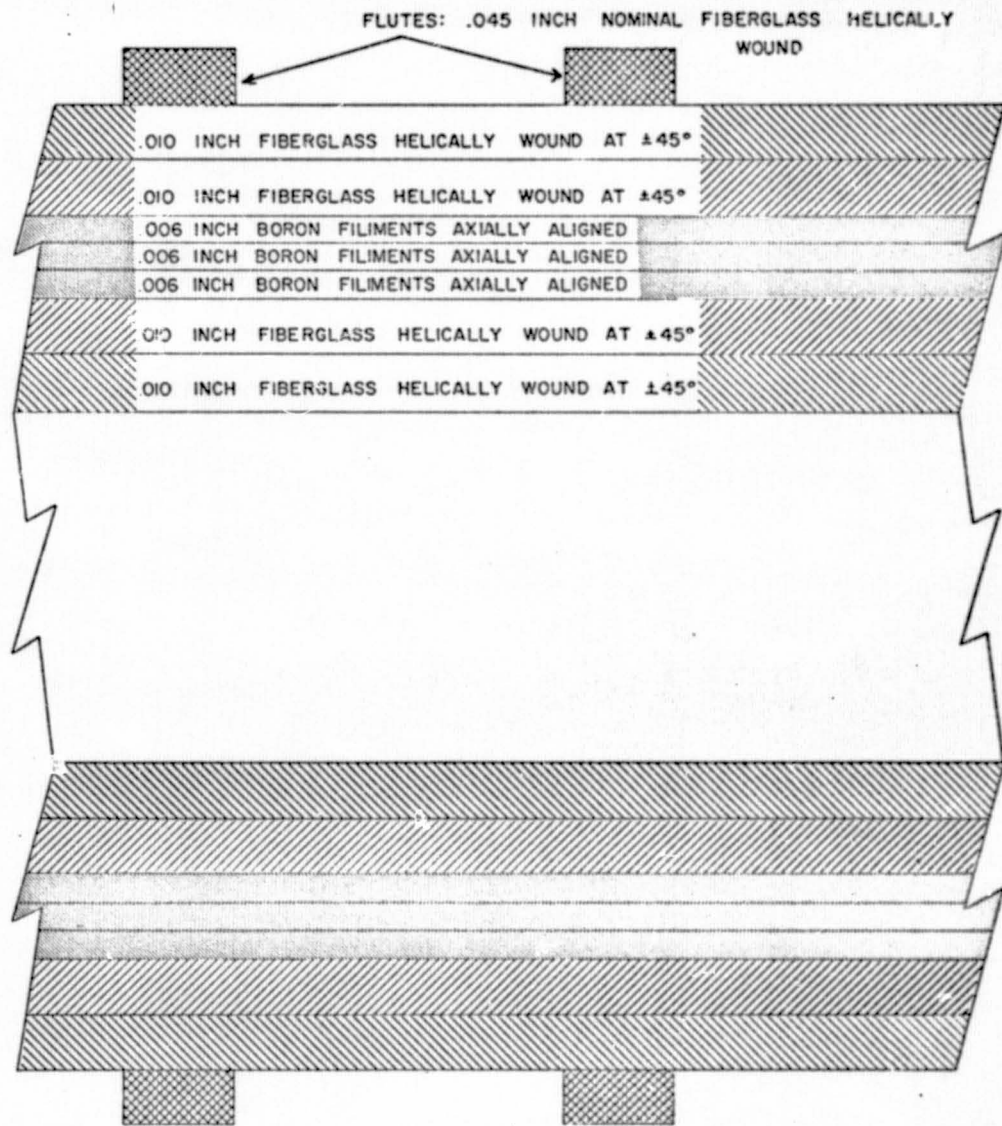


FIG. 2

| | | | |
|--|-----------|--|-------------|
| Material | AS NOTED | Lamont Geological Observatory of Columbia University Palisades New York | |
| Finishes | | BORON FILIMENT DRILL STEM STRUCTURE | |
| Scale | NONE | Drawing | |
| UNLESS OTHERWISE SPECIFIED DIMENSIONS ARE IN INCHES AND INCLUDE PLATING | | | |
| TOLERANCES | | | |
| | FRACTIONS | DECIMALS | ANGLES |
| xx | ±.015 | ±.0012 | ±.1° |
| xxx | ±.005 | ±.00012 | ±.05° |
| Drawn | S. KAGHAN | Checked | R. S. PERRY |

at plus and minus 45° to the stem axis. Three layers of boron filaments are wrapped over these layers that are aligned with the long axis of the tube. Two additional layers of fiber glass are wound over the boron at angles plus and minus 45° to the stem axis. This configuration gives a nominal outer diameter of 0.990" with an inner diameter of 0.875".

The flutes to transport drill cuttings to the surface are helically wound around the stem body as shown in Figure 1. The flutes are also made of fiber glass and form a double helix with a 1" pitch. The outer surface of the flutes are impregnated with silica powder to increase abrasion resistance. Each flute is 0.10" to 0.15" across and stands about 0.45" above the stem body. As can be seen in Figure 1, the diameter of the stem body is increased at the female joint, whereas the flute diameter is constant, and as a result the flute depth over the joint area is very small, i.e., about 0.01".

(b) Physical characteristics determined from tests: Mechanical tests were made on some prototype tube sections fabricated at the AVCO Corporation. These tubes differed slightly from the tubes described above. The configuration of the AVCO tubes is as follows:

- (i) 0.014" plus and minus 45° epoxy-glass inner layers.
- (ii) 0.015" axially aligned boron.
- (iii) 0.011" plus and minus 8° fiber glass outer layers.

The average measured properties of several tube sections were: Axial Young's Modulus 11.6×10^6 PSI, shear modulus 1.57×10^6 PSI and Poisson's ratio 0.20. (The AVCO Corporation's final report is appended to this document, APPENDIX A.) Theoretical values predicted were 12×10^6 PSI and 1.3×10^6 PSI for the Young's and shear moduli.

AVCO also conducted tests to determine the wear resistance of the flutes with different "fillers" in the epoxy fiber glass. Three fillers were

tested; graphite powder, teflon, and chopped silica. The chopped silica produced the greatest improvement in wear resistance. (See the AVCO report for further details.)

The thermal conductivity of the test specimens made at AVCO were measured by that company. Conductivity was measured as a function of temperature. The only results relevant to the HFE are those at 37.7°C and 93.3°C. They are 0.0276 and 0.467 watts/cm/°C, respectively.

Further conductivity measurements on the boron stem were made at ADL by request of L-DGO under Subcontract #6. These measurements are reviewed in the ADL report, APPENDIX B.

These results give a value of conductivity equal to 0.0096 watts/cm°C at 27°K and 0.0108 watts/cm°C at -73°K. The procedure of the AVCO conductivity measurements was not made available to L-DGO so that we have no way of assessing the difference by a factor of two between AVCO and ADL numbers. We did witness the tests at ADL and reviewed the analysis so that we have confidence in the results. We conclude that the conductivity of the boron tube is:

| °C | °K | Conductivity* |
|-------|-------|---------------------------|
| 27°C | 300°K | 0.0096 ± 0.001 watts/cm°C |
| -73°C | 200°K | 0.0108 ± 0.002 watts/cm°C |

* The conductivity is measured axially in the tubes.

(c) Drilling Tests:

The prototype samples made by AVCO were used to compare the boron reinforced fiber glass stem with the titanium stem. These tests were carried out in the Martin Marietta Corporation facility in Baltimore. These tests gave an early indication that the stem could transmit the required percussive energy.

In the spring of 1968 we built a small test facility at L-DGO. The facility consisted of a Black and Decker rotary-percussive drill, Model 723, that has characteristics very similar to the ALSD, and some test specimens such as finely crushed basalt stone, and blocks of vesicular and dense basalt. All of the tests described here were made in the L-DGO facility.

A comparison of drilling rates was made using samples of titanium, boron reinforced epoxy fiber glass, and fiber glass stems reinforced with axially aligned glass filaments. Each of the fiber glass stem samples were composed of two 20" lengths bonded together over an aluminum plug. The titanium stem sample was 34" long (2 sections of standard ALSD stem).

Table 1 shows the results of tests with the three types of stem. Notice the tests were run for four different types of drill bits as well. (The drill bit tests will be discussed later.) For both the solid-face and coring bits with a diameter of 1.027" the drilling rates achieved with the three stems are comparable (the 0.53 rate for axially aligned glass fiber maybe anomalous, perhaps due to an exceptionally hard layer in the basalt.) The energy transmission of each is better tested by the larger diameter bits where more energy per blow is required because of the large cutter contact area. For these tests the boron filament reinforced fiber glass and the titanium show a decided advantage over the glass. We believe that larger kerf areas might also simulate the performance with a 1.027" diameter bit when the drill stem length is nearly 10 feet.

The axially aligned glass performs remarkable well considering the low modulus of the material. However, it is apparent that long lengths of this material might produce very slow penetration rates.

TABLE 1: Drilling rates (in inches/minute) of development
ALSD bits as a function of kerf area* and type of drill stem.**

| Type of Bit | Solid Face (1.027" dia.) | Coring (1.027" dia.) | Coring (1.125" dia.) | Coring (1.250" dia.) |
|---------------------------------|-----------------------------|-------------------------|-------------------------|-------------------------|
| Kerf Area | 0.821 in ² | 0.391 in ² | 0.558 in ² | 0.789 in ² |
| <u>Type of Stem</u> | | | | |
| Titanium | 0.84 (1) | 1.10 (1) | 0.65 (1) | 0.46 (1) |
| Axially Aligned Glass Fibers | 0.82 (2) | 0.53 (1) | 0.44 (1) | 0.26 (1) |
| Boron Reinforced Fiber Glass | 0.99 (2) | 1.20 (1) | 0.71 (2) | 0.32 (1) |

Notes:

- The number in parentheses gives the number of tests conducted. When two tests were made, the results were averaged.
- Tests are based on drilling one minute.
- All the tests were made in dense basalt.

* Width of the bite of the cutters times the mean circumference.

** These data are plotted in Figure 3 on the following page.

DRILLING RATE VERSUS BIT KERF
AREA IN DENSE BASALT

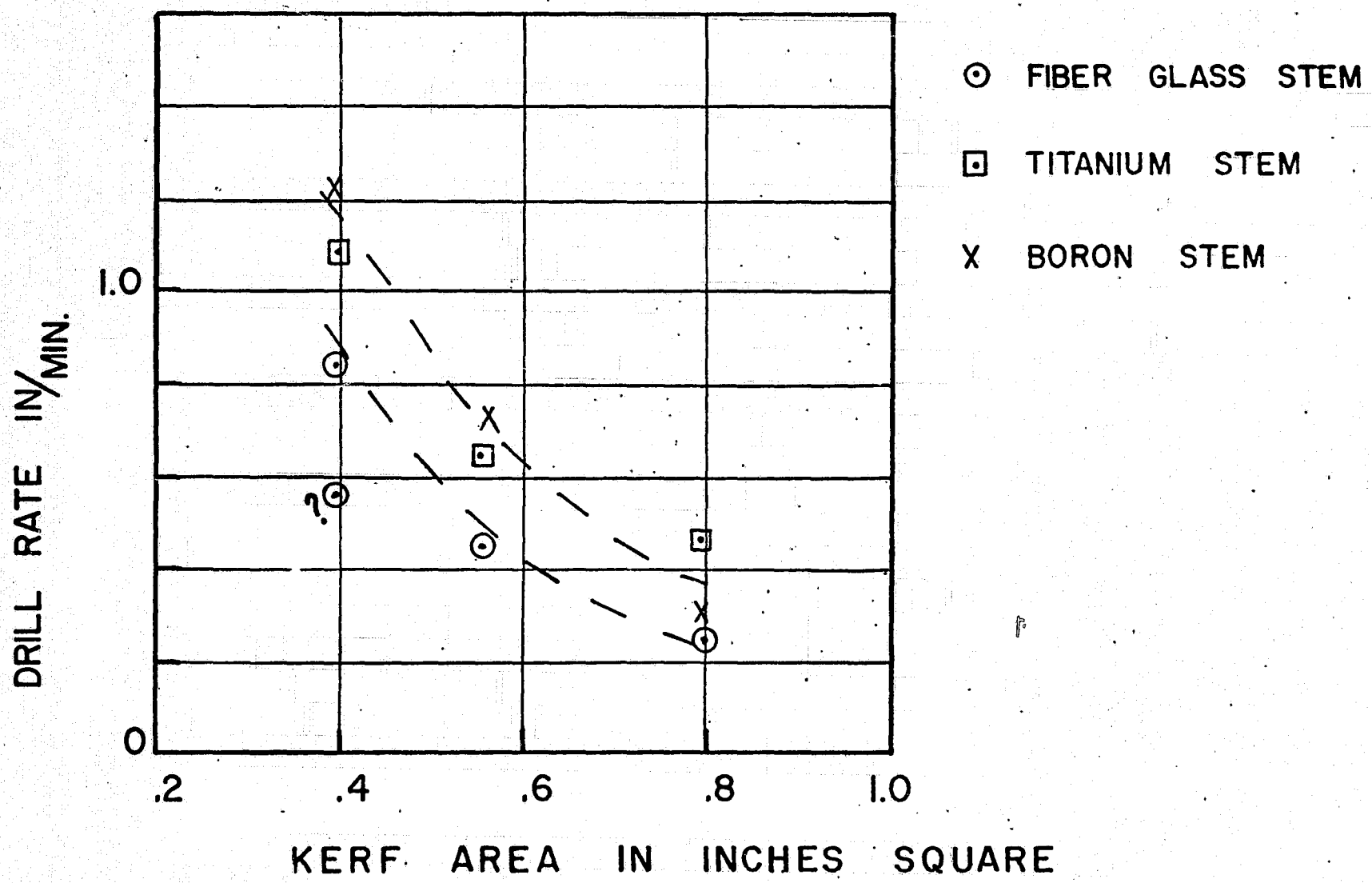


FIG. 3

2. Taper Joint:

(a) Design history: Designing a workable taper joint for the boron filament drill stem proved to be the most difficult task in the development of the boron drill stem. The initial taper joint design was a simple taper of 0.012inches/inch for a length of 1" machined into the outer glass layers of the male and female pieces. The inner part of the tube containing the boron filaments was ground to form a flat shoulder that butted when the joint was made up. This type of joint failed during testing due to lack of adequate hoop strength; also the boron filaments sheared off at the shoulders.

To correct for this, the second design incorporated steel rings; one internally on the male to retain the ends of the boron filaments and the other externally on the female section to increase the hoop strength. (See the drawing in APPENDIX A, Figure 2.) This joint also failed after a brief test because of insufficient hoop strength. The last joint mentioned was remachined to relieve the stress at the glass-boron interface, but this modification allowed the slip in rotation, joints overheated and collapsed. (See APPENDIX C; "Drill tests during January, 1969, pp. 2 and 3, for more detailed descriptions of these tests.)

(b) Final design of the taper joint: The previous tests led to a basic revision of taper joint design. The steel reinforcing rings were removed, and the female taper was reinforced by overlaying it with short lengths of boron filaments. In addition, circumferentially wound fiber glass was applied around the female taper joint to increase hoop strength. The taper angle was increased from 0.012 inches/inch to 0.018 inches/inch to decrease radial stresses in both the male and female sections of the taper. This joint configuration has proven successful, and is the

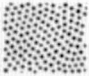

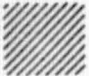
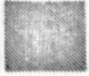
basis for the final design. The configuration of glass and boron layers in the final taper joint design is shown in Figures 1 and 4.

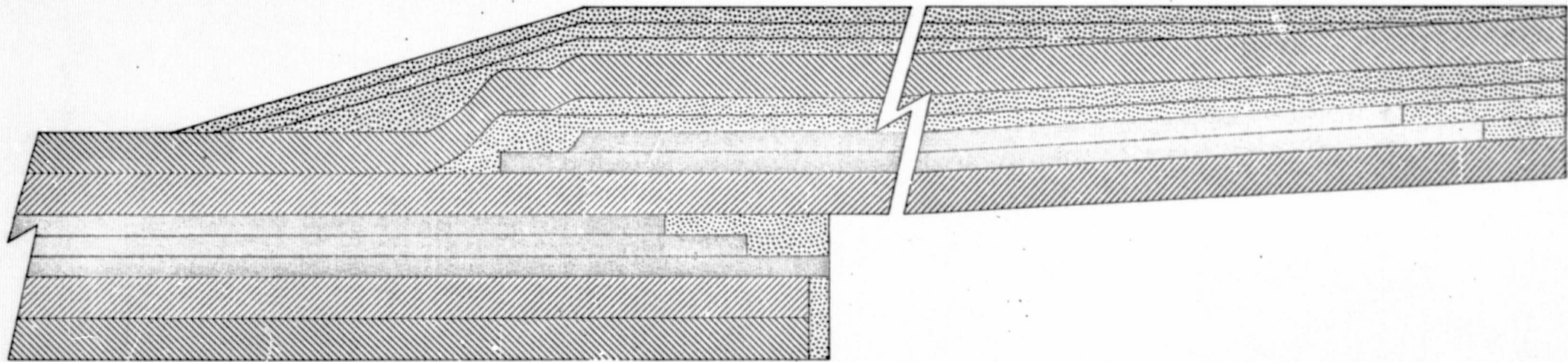
(c) Summary of taper joint tests: Many tests of the taper joints were made in the course of development. For the final taper joint design we ran an endurance test that lasted for 22 minutes of drilling in dense basalt with no apparent joint degradation.

3. Bit Adapter Section: It was found necessary to put a 4" titanium adapter section between the drill stem and drill bit to allow for the interchangeability of drill bits, to decrease temperatures seen by the epoxy stem, and to reduce abrasion in the section behind the bit. Figure 1 shows the detail design of the bit adapter.

(a) Thermal considerations and tests: It was felt that there may be a significant amount of heat generated in the drill bit during drilling of rock. Concern for the effect of this heat on the resin system of the boron filament stem led to a test to determine the magnitude of the problem. The test is described fully in APPENDIX D and is summarized briefly below. The temperature measuring system employed three copper constantin thermocouples, a strip chart recorder, ice bath, insulated thermocouple housing and other associated equipment.

Using a Black and Decker Model 723 power head and the boron drill stem with a 1.027" solid-face bit, dense basalt was drilled for a given length of time (1 to 4 minutes); at the completion of the drilling period the bit was transferred to an insulated thermocouple housing and temperature readings at various points on the drill stem were made. The temperature as a function of drilling time is shown in Figure 5. It can be seen that even after 4 minutes the bit temperature is about 90°C which is well above the point at which the epoxy degrades.

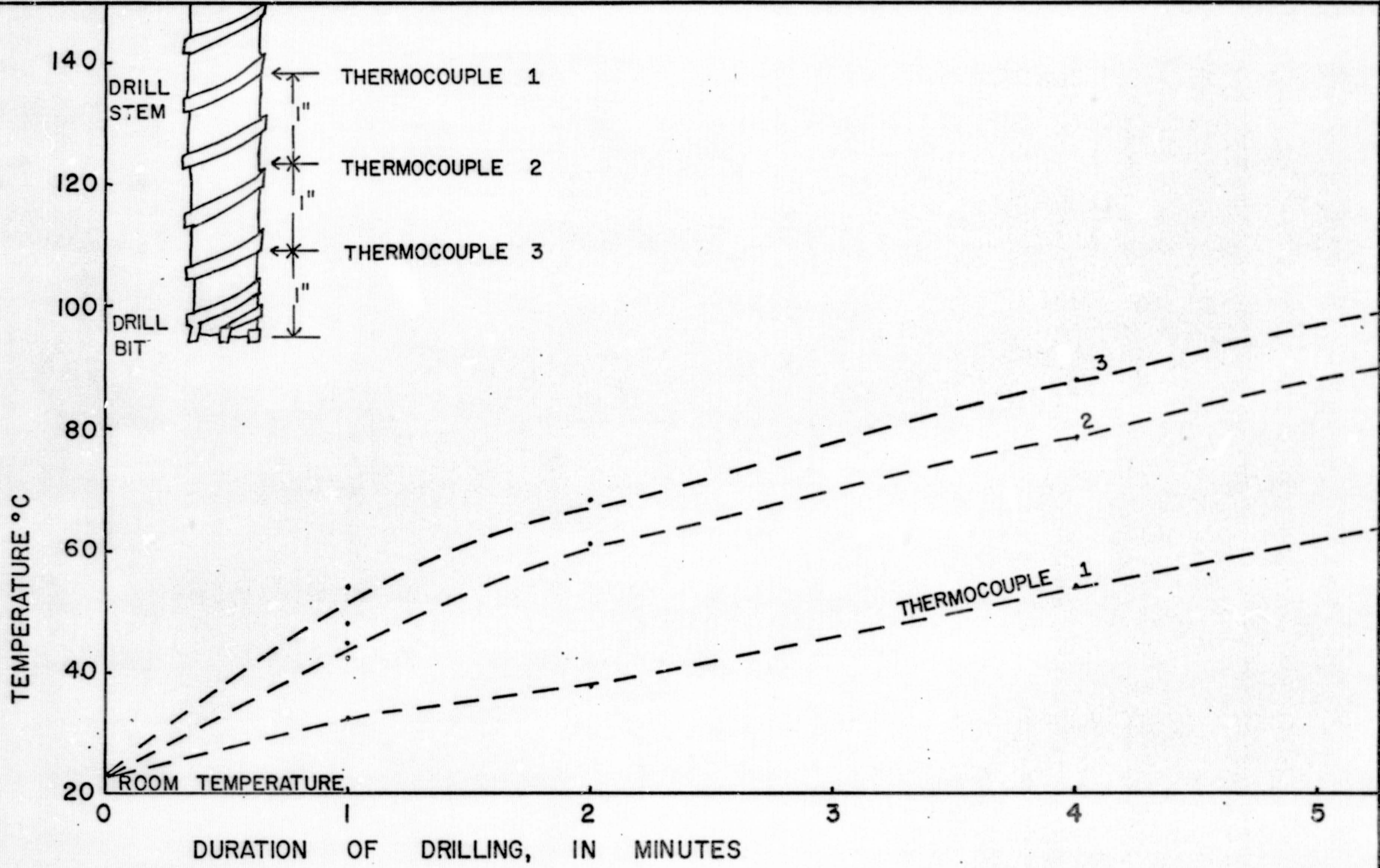
-  .005 INCH FIBERGLASS CIRCUMFRENTIALLY WOUND
-  .010 INCH FIBERGLASS HELICALLY WOUND AT $\pm 45^\circ$
-  .010 INCH FIBERGLASS HELICALLY WOUND AT $\pm 45^\circ$
-  .006 INCH BORON FILIMENTS AXIALLY ALIGNED



CENTER LINE

FIG. 4

| | | | |
|--|-----------------------|--|----------|
| Material | AS NOTED | Lamont Geological Observatory of Columbia University Palisades New York | |
| Finish | X | | |
| Scale | NONE | | |
| UNLESS OTHERWISE SPECIFIED DIMENSIONS ARE IN INCHES AND INCLUDE PLATING | | | |
| TOLERANCES | | | |
| DECIMALS | FRACTIONS | ANGLES | |
| XX | 015 OVER 12 INCHES TO | 1/2 | |
| XXX | 005 OVER 12 INCHES TO | | |
| Drawing | | | |
| Drawn | S KAGHAN | Checked | RS PERRY |



BIT TEMPERATURE RISE VERSUS DRILLING TIME IN DENSE BASALT

FIG. 5

(b) Adapter design: As a result of the tests described above a nominal length of 4" was chosen for the bit adapter. The size of the drill bits and boron drill stem determined the other dimension of the bit adapter.

B. Solid-Face Bit

1. Experience gained in developing the ALSD coring bit provided information on bit design parameters. Point pressure exerted on the rock by the carbide kerf cutters must be kept above a finite threshold value to obtain chipping at the rock face. If point pressures are below the threshold, the rock is pulverized rather than chipped and the drilling rates will be much lower than those obtained with the LASD bit.

2. The design basis of the solid-face bit was the ALSD coring bit. In the first solid bit design a single tungsten carbide blade was placed inside the bit shell to remove the core. On the first prototype this blade protruded beyond the kerf cutters. (See Figure 6.)

Drilling rates obtained with this bit were extremely low because of low point pressures. A second test was made with this bit to determine the efficiency of the core cutter. An ALSD coring bit was used to drill a hole in dense basalt, leaving the central core undisturbed. This hole was re-drilled with the solid-face bit as a test of core cutter efficiency. The central core was removed at a high rate. This test showed that it is relatively easy to break up the central core once it is standing about 1/2 inch above the cutting face. The reason for this is that the free cylindrical surfaces lead to fracturing of the column both in shear and spallation. This discovery led to a final, highly efficient solid-face bit design.

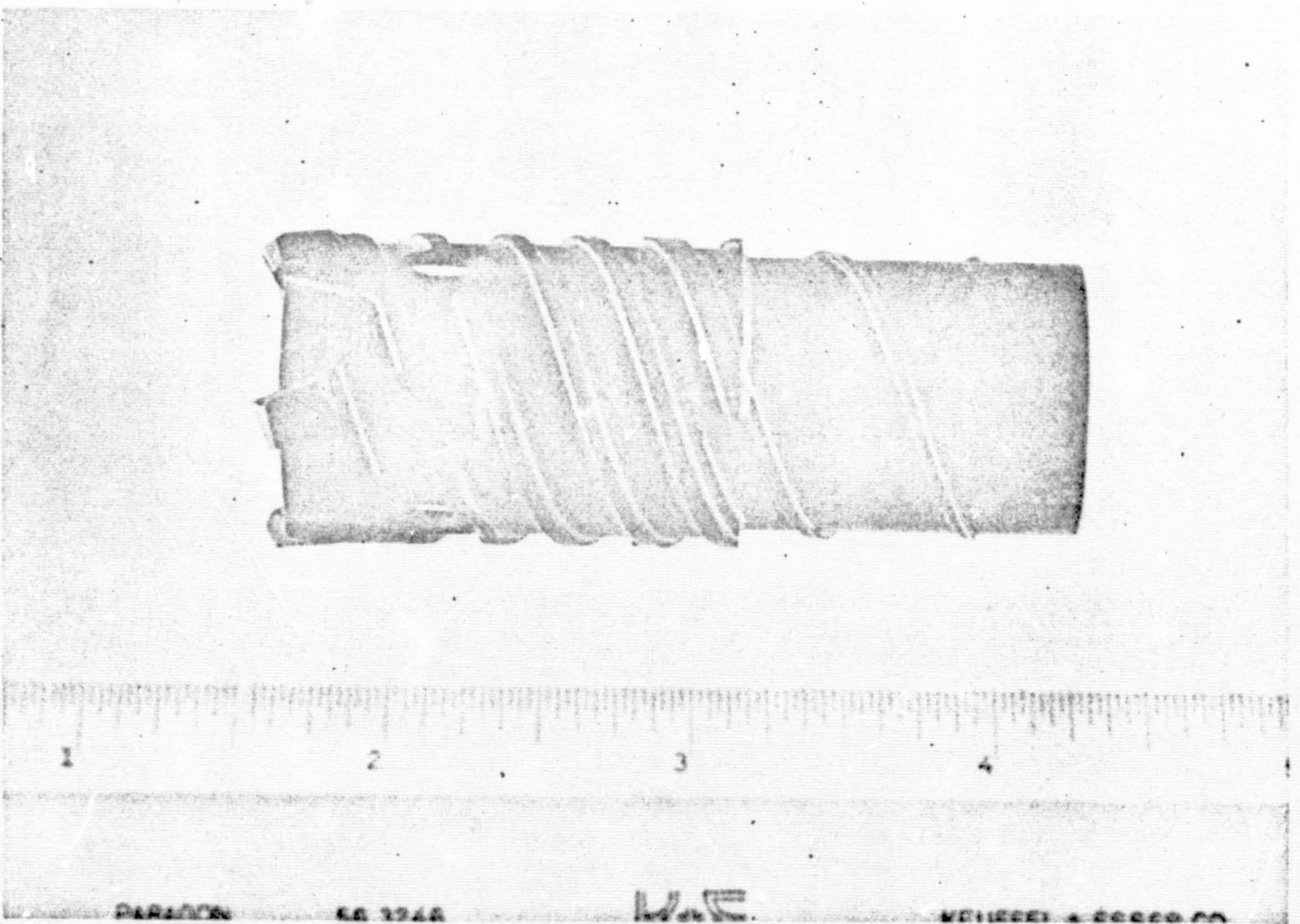
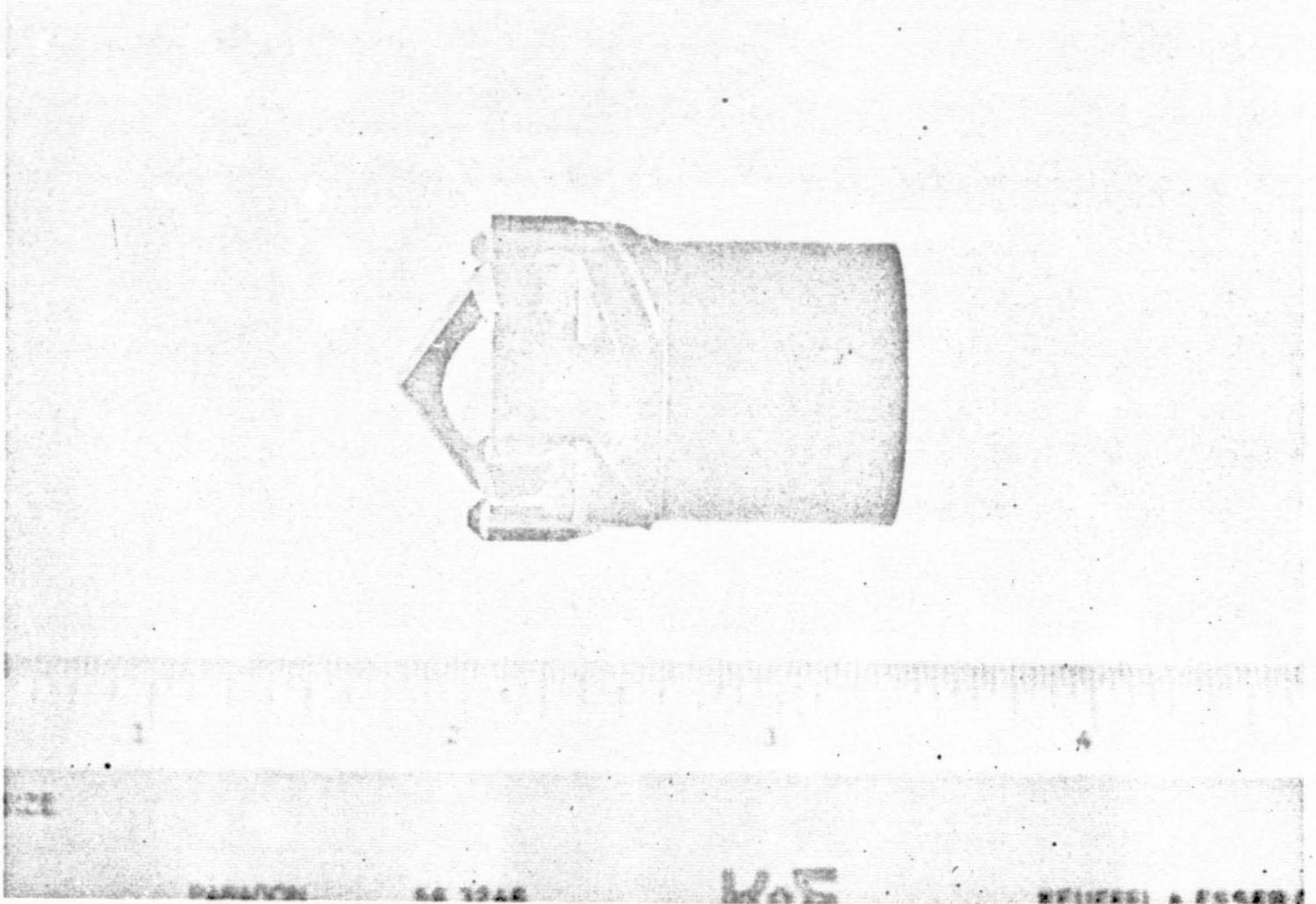


FIG. 6 - Prototype of solid faced drill bit. Note the core cutter protruding beyond the kerf cutter at left.

FIG. 7 - Solid faced drill bit, final design. Three of the six elliptical exit ports for core cuttings are visible.

The second prototype solid-face bit also used the ALSD coring bit. However, the blade was recessed about 3/8 of an inch behind the keff cutters of the core bit. Six elliptical holes were machined into the body of the bit at the base of the core cutter to serve as exit points for the core cuttings. (See Figure 7.)

Tests of this bit were successful, giving rates of 4 inches/minute in vesicular basalt and 1 inch/minute in dense basalt. (See Table I.) This bit configuration has been chosen for the flight hardware with only minor modification.

One important consideration of the bit design was reduction of the kerf width of the annular coring cutters. Experimental results (given in Table I and plotted in Figure 5) obtained with bits of three different kerf areas, show an almost linear relation between kerf width and drilling rate. The great gain in effective kerf area of the solid-face bit is dramatically shown by these tests.

C. Core Retrieval System:

1. System Concept: The core retrieval system is designed to collect a subsurface core sample without the necessity of removing the drill stem from the borehole. This is accomplished by locking a core liner tube into the lower end of the drill stem, drilling to a depth approximately equal to the length of the core liner tube and then removing the tube.

A typical procedure for coring one hole would be to attach one of six core liner tubes to the core locking mechanism. This assembly is inserted in the drill string with an emplacement retrieval tool and locked in place by rotating the core lock capstan. The hole is drilled to a depth calculated to fill the core liner tube, the core lock is released, and the core

liner tube is removed by using the retrieval tool. The sequence is then repeated until drilling is completed. Figure 8 shows the complete coring system developed at the Lamont-Doherty Geological Observatory.

2. Core Liner/Sample Return Container: The core liner was designed to function as both a core liner and a sample return container. Strict design requirements are placed on it as a result of this dual function. The core tube must interface with the drill stem, core lock and sample return container and meet the aseptic requirements for returning lunar samples.

The prototype core liner is fabricated from thin-wall, high strength aluminum alloy tubing. Testing of early designs showed that the tubes were deficient in two areas: (1) The presence of rock particles which became lodged between the core tube outer surface and the inside of the drill stem made removal of the core assembly difficult, and (2) core material was frequently lost during removal of the liner from the stem.

Core liner jamming was eliminated by installing a felt-flocked paper seal at the bottom of the core liner (see Figure 9). This seal effectively limits the entry of rock and rock dust particles into the core liner-drill stem interface and cleans that interface during core liner insertion.

Loss of cored material was minimized by using a core liner fitted with a core catcher. The use of fine wires radially aligned to the long axis of the tube functioning as core catcher proved somewhat successful. However, a disc of mylar film (shown in Figure 10) cut into 12 triangular segments proved to be the most effective core retainer tested to date in dry rock powders. The core catcher is held in place between butting shoulders of a separate tip section. The core catcher disc is fabricated with a diameter large enough to fit in this shoulder and is held in place by the clamping action of the two pieces.

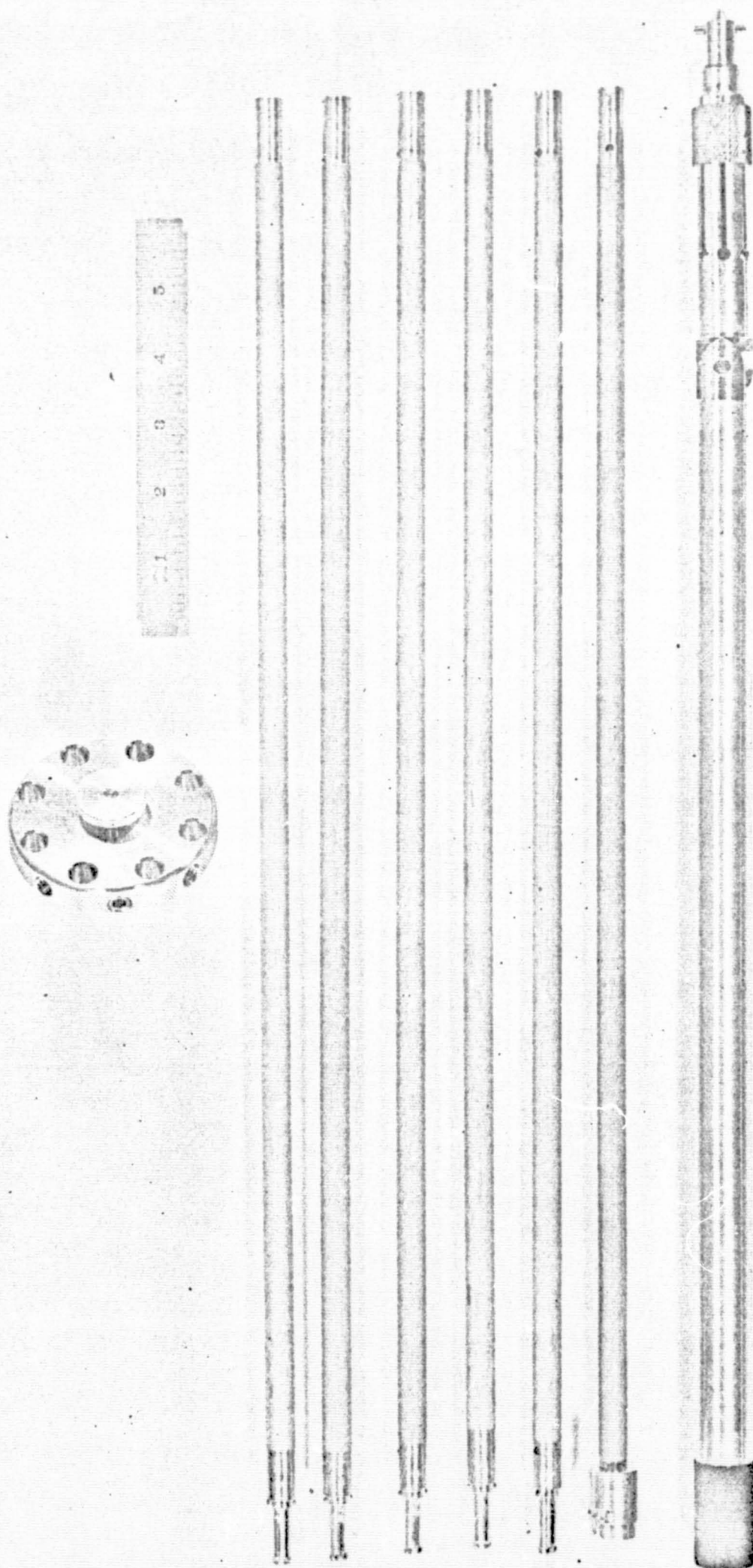


FIG. 8 - A set of coring equipment. From left to right; torque limiting handle for emplacement retrieval tool, five extension sections for emplacement retrieval tool, interface adapter section, and the core lock - core liner assembly.

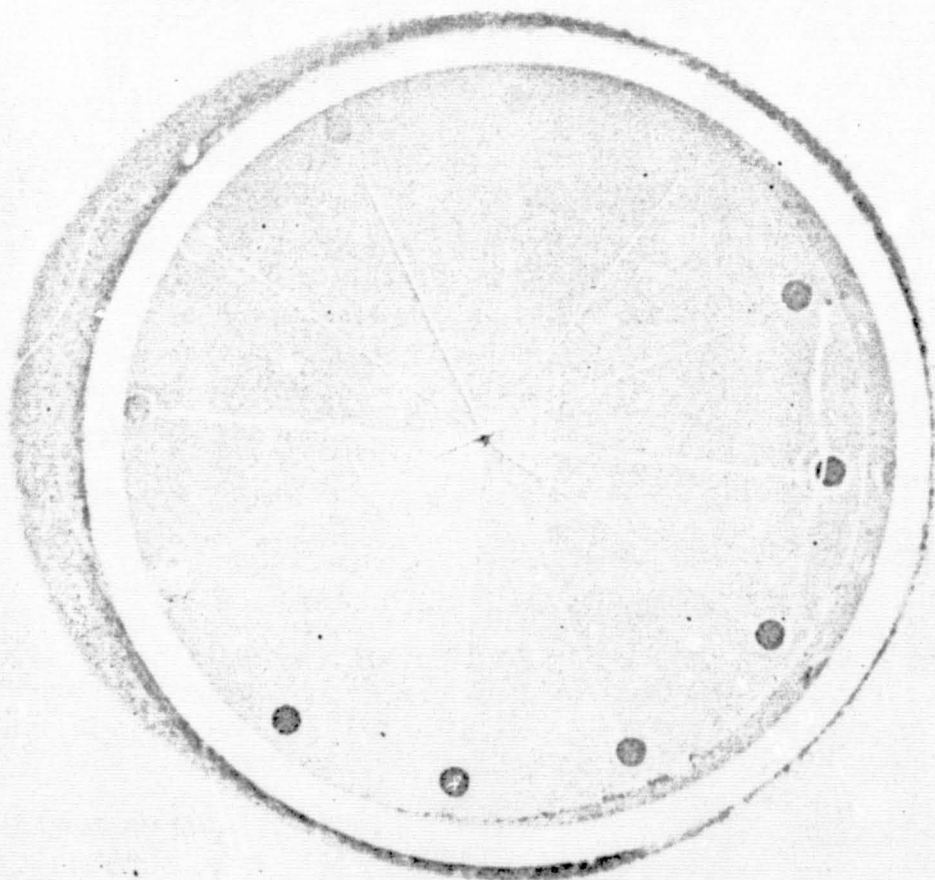
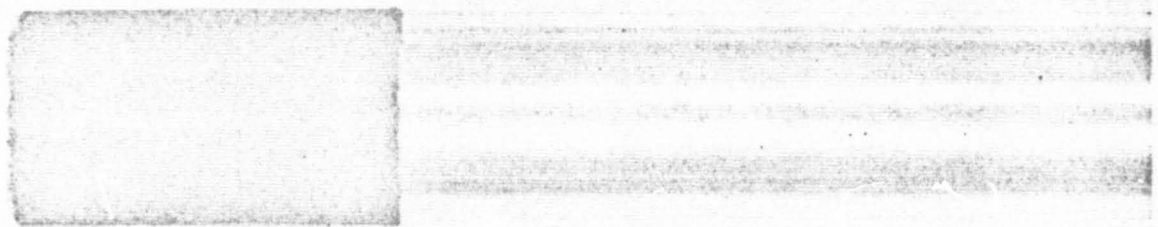
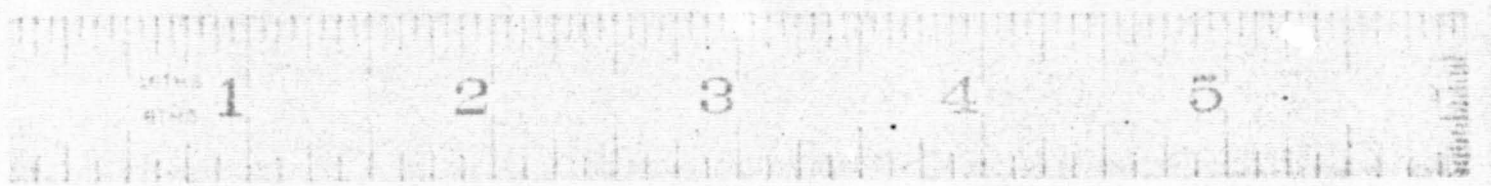


FIG. 9 - The felt flocked paper seal winch prevents entry of rock particles into the core liner - drill stem interface.

FIG. 10 - A mylar film core catcher shown mounted in a core liner sample/return container.

3. Core Lock: The function of the core lock is to hold the coring assembly in place during the drilling operation.

Our initial core lock design utilized phosphor bronze spring fingers which were forced against the drill stem wall at an acute angle. A screw driven cam actuated the spring fingers. Upward force on the coring assembly caused the spring fingers to slightly penetrate the drill string wall thereby preventing movement of the coring assembly. Tests showed that these fingers were not nearly strong enough to hold the core liner in place.

A second development core lock used a ball detent mechanism. Two 0.250" diameter steel balls were contained in the core lock body. Detent holes were made in the drill stem wall to accommodate the steel balls. A screw driven cam forced the balls outward into the detent holes. Reversal of the cam motion allowed the balls to retract during core retrieval. Tests in dry rock powders revealed that the core liner exerted such a strong upward force during drilling that the steel balls actually tore the fiber glass stem upward from the detent holes.

A third and final core lock design utilized an expandable cylinder with a knurled surface to engage the interior surface of the stem. The first model of this type had two tapered plugs enclosed in an articulated cylindrical shell. A lead screw drew the plugs together causing an increase in the diameter of the shell. A theoretical mechanical advantage of over 500 is possible. In the final design a simpler version of this core lock utilizes only one taper plug and is articulated at only one end. The final core lock design is shown in Figures 11 and 12. Figure 13 shows a final assembly drawing of the core lock mechanism.

The core lock and core liner are joined with a knuckle type joint mated by rotating one of the pieces through a 90° arc, pictured in Figure 14.

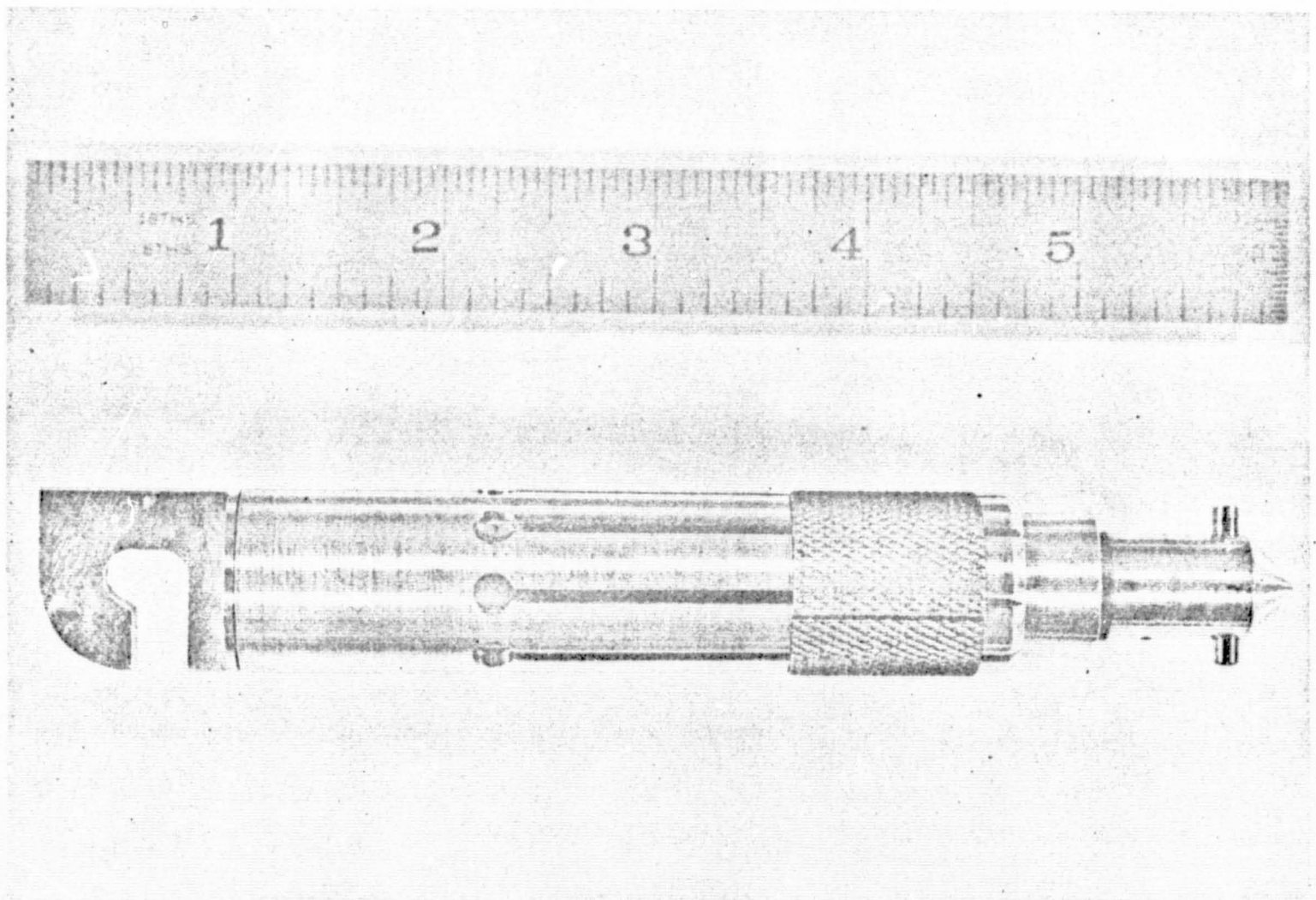
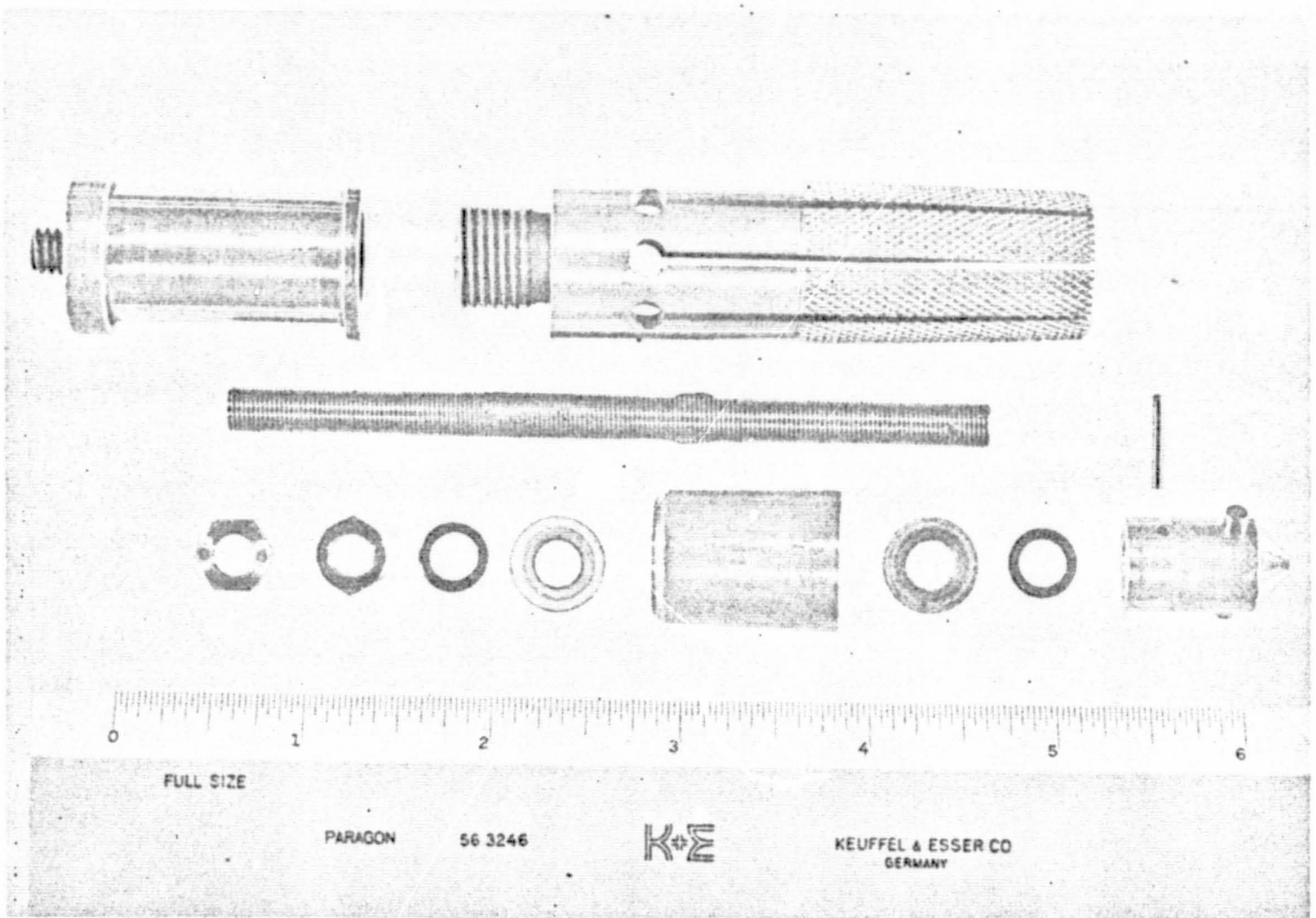


FIG. 11 - Parts of a Prototype core lock of a design similar to the final design.

FIG. 12 - The final design core lock with half of knuckle joint attached. Note the separate knurled sleeve.

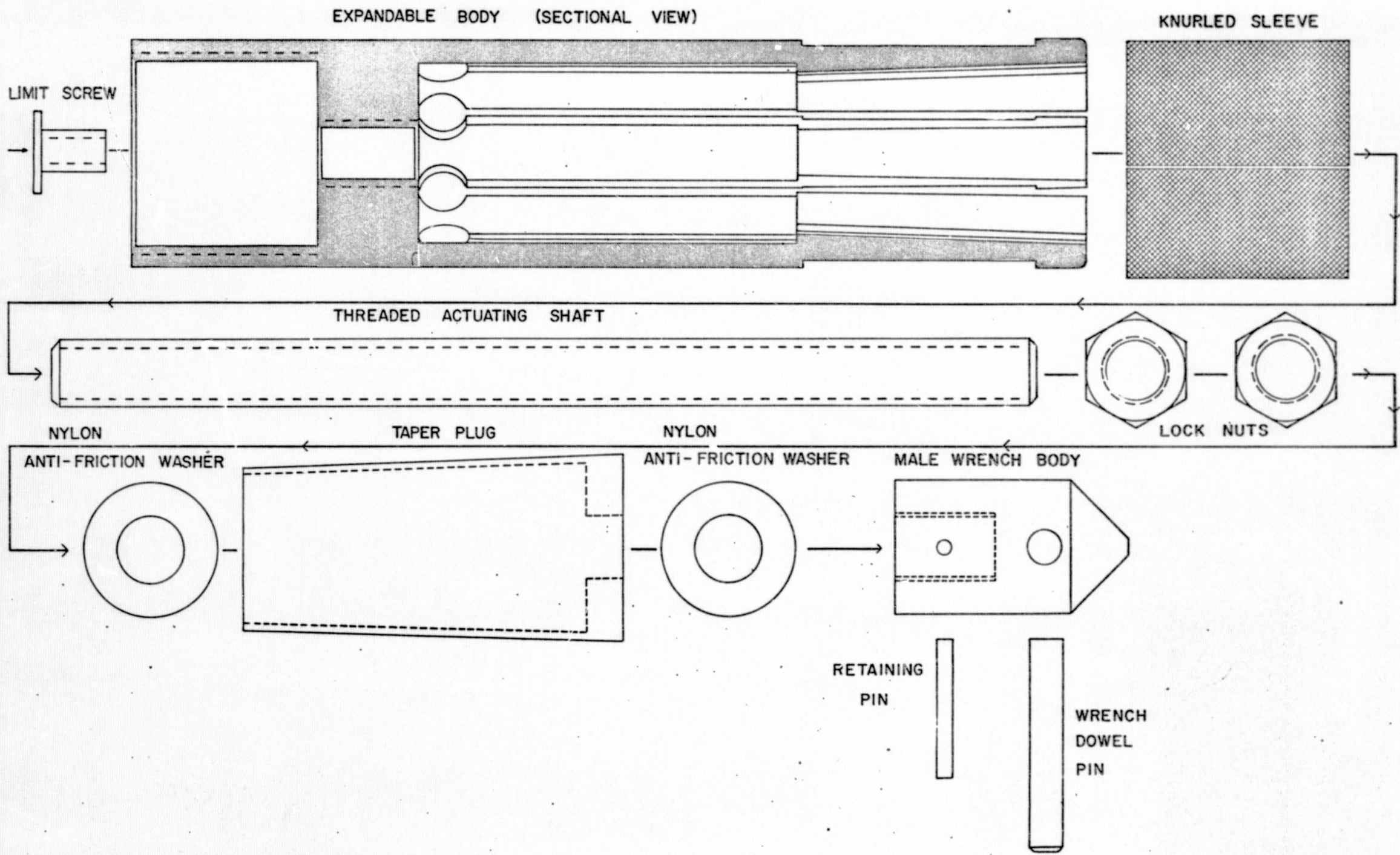


FIG. 13

| | | | |
|--|-------------------------------|--|--------|
| Material AS NOTED | | Lamont Geological Observatory of Columbia University Palisades New York | |
| Finishes | | CORE LOCK ASSEMBLY DIAGRAM | |
| Scale NONE | | Drawing | |
| UNLESS OTHERWISE SPECIFIED DIMENSIONS ARE IN INCHES AND DECIMAL PLACING | | | |
| TOLERANCES UNLESS OTHERWISE SPECIFIED | | | |
| FINISHES | SHAFT TOLER. | ANGLES | |
| XX | 0.15 (H9/D9) 12 (H7/d7) 1.12 | 1.2 | |
| XXX | 0.05 (H8/d8) 1.2 (H8/d8) 1.12 | | |
| Drawn | Checked | Date 9/26/69 | Welder |

REPRODUCIBILITY OF THE ORIGINAL PAGE IS POOR.

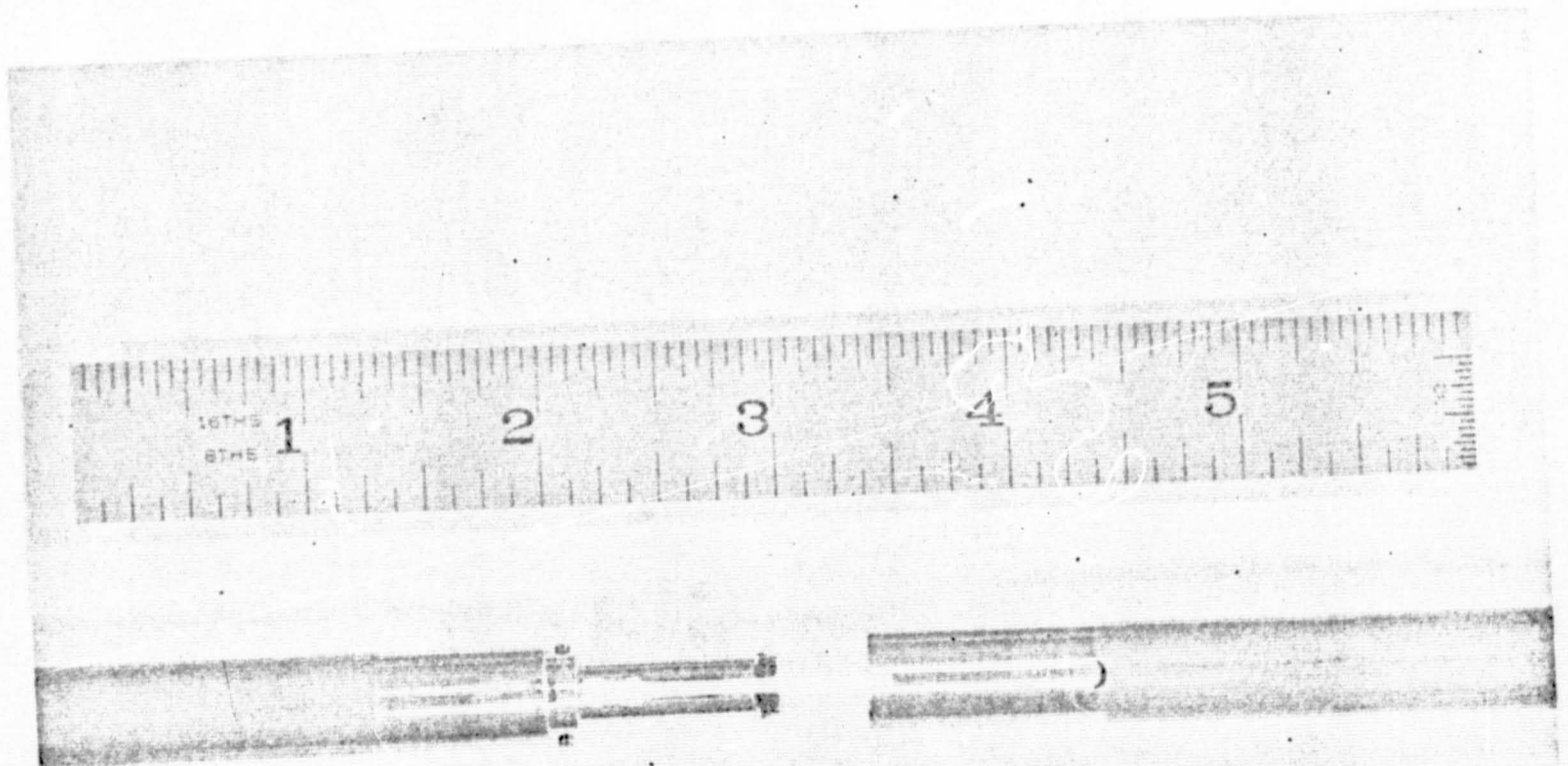
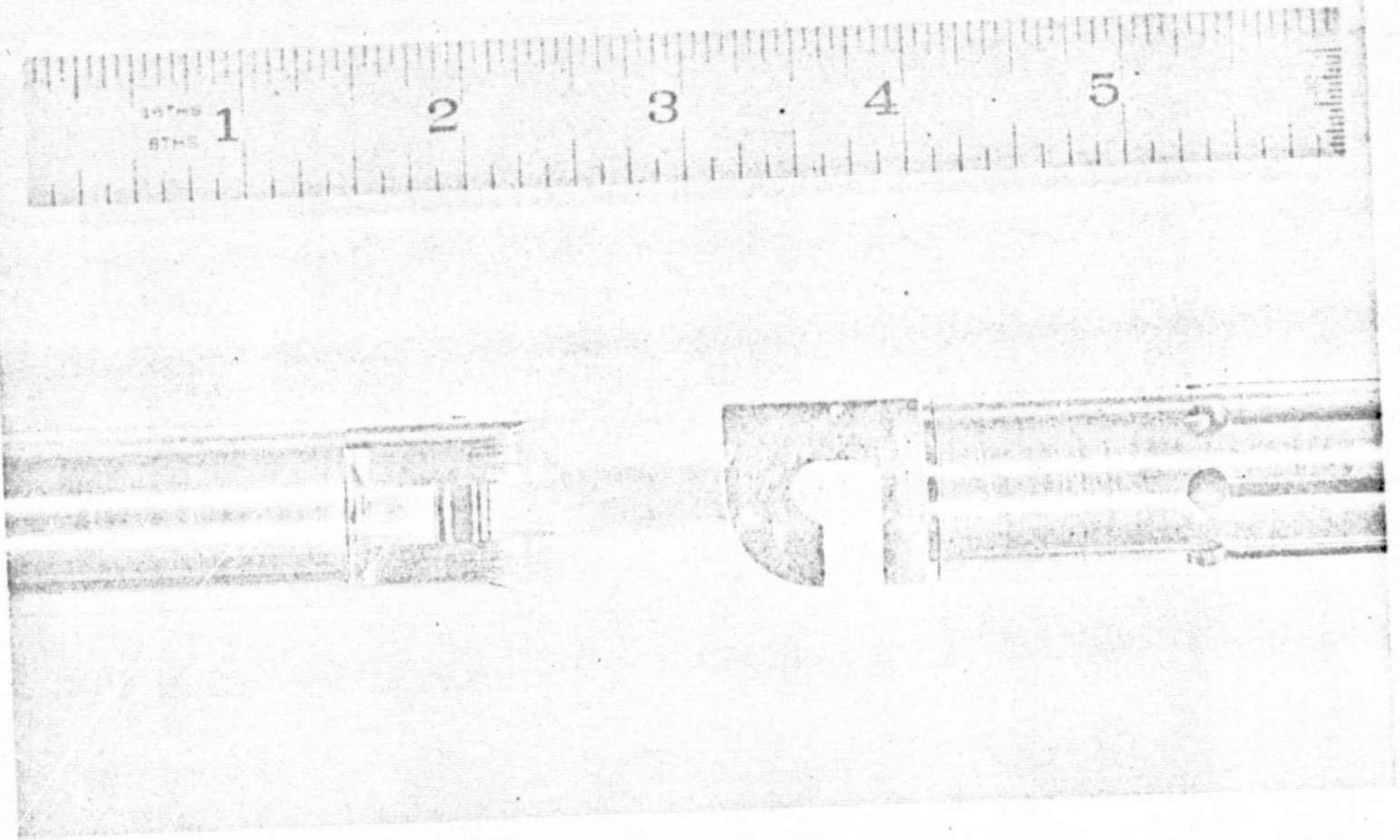


FIG. 14 - The knuckle joint, core liner tube on left and core lock on right.
FIG. 15 - Locking joint of Emplacement Retrieval Tool. This joint transmits tension compression and torque.

4. **Emplacement/Retrieval Tool:** Emplacement, retrieval and core lock actuation are performed with a special tool. This tool must be designed to transmit tension, compression and bi-directional torque to the core lock capstan. The prototype unit consists of a torque-limiting handle, five extension sections, and one adapter section. The handle is connected to the adapter section directly or with one to five extension sections interposed. The interstem joints are not separable once they have been connected except with a special tool. Ordinarily there is no need to separate the sections on the lunar surface.

The handle limits the torque applied to the core lock to a pre-set amount. The components of the core emplacement and retrieval tool are shown in Figures 15 and 16.

5. Summary of Development Tests of the Core Retrieval System:

Development tests were carried out at the L-DGO test facility using a Black and Decker model 723 rotary hammer run at a reduced voltage to simulate the ALSD power head. A fifty-five gallon drum filled with material from the Martin Marietta Corporation was used to simulate the lunar surface. Hard rock drilling was done in either a 17-inch thick block of vesicular basalt or an 8-inch thick block of dense basalt. Tests were run using the core system pictured in Figure 8 in a very loose mixture of basaltic rock powders. The predominance of the material was finer than 74μ (over 50%) but coarser particles were also included up to $1/4$ " across. The system was shown to take a representative sample of the powders penetrated, however, the amount of sample retained was a strong function of drilling rate. For example, drilling at a rate of 4 inches per second the core recovered only 15% of the material penetrated that was above the core catcher. But at 2 inches per second and 1 inch per second the percent recoveries were about 35% and 75%, respectively. These results show that for effective

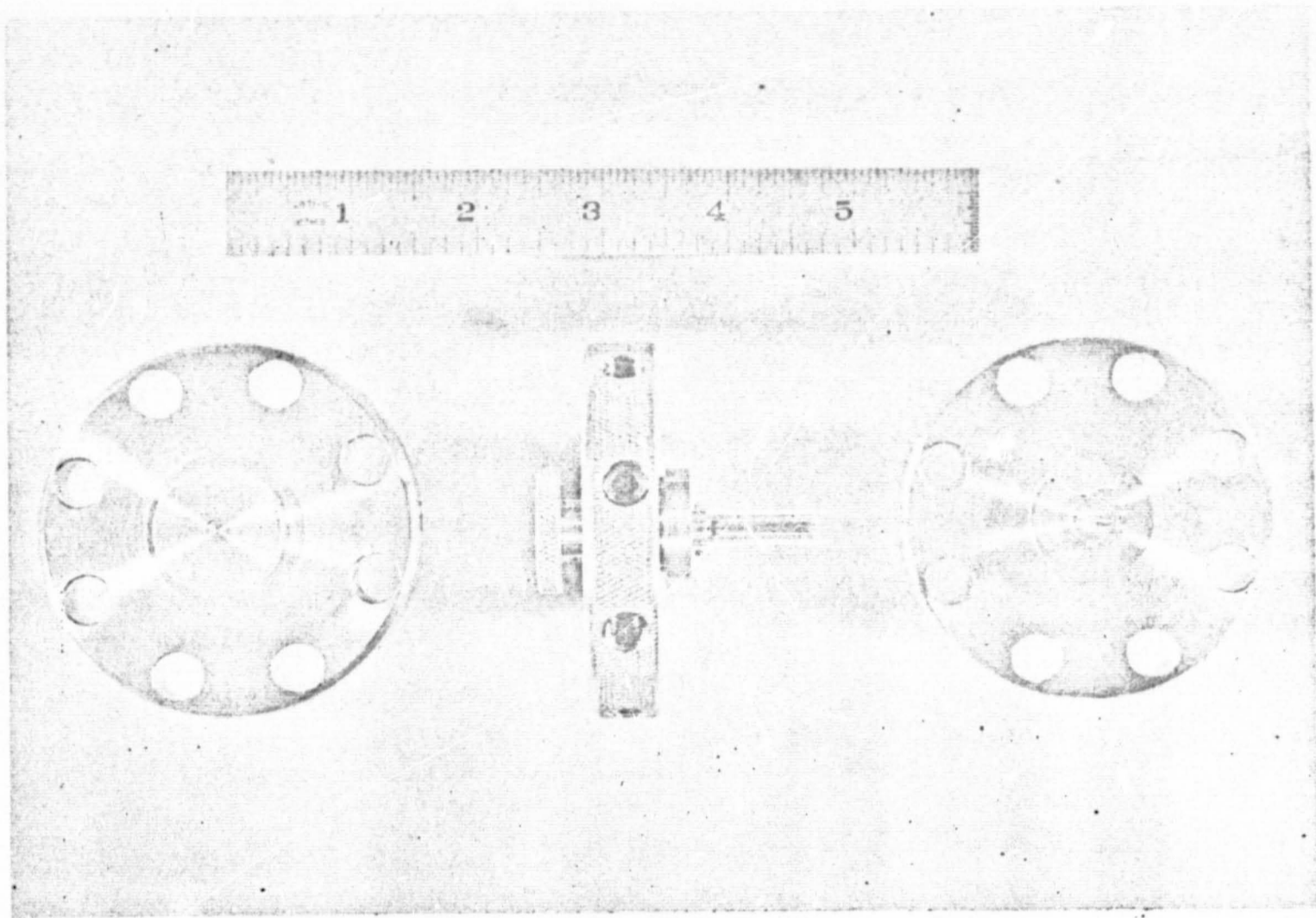


FIG. 16 - The torque limiting wrench handle. From left to right are the top, side and bottom views. The side view shows the actuating pin with handle and three of eight recess holes for the ball detents.

sampling of a loose material such as the lunar regolith, the return is greatly improved by keeping the penetration rate below 1 inch per second, or about one section of stem per 30 seconds.

ITEMS DELIVERED UNDER THIS PROGRAM

A. Four sets of boron filament drill stem manufactured by the Arthur D. Little Company are deliverable to the Martin Marietta Corporation. Each set consists of five standard stem sections and one adapter section. The stems will conform to L-DGO drawings; BFS 1000 Rev. A, BFS 1001 Rev. A, and BFS 110 Rev. A (information included in Figure 2).

B. Ten solid-face drill bits which will interface with the adapter were fabricated by Chicago-Latrobe for L-DGO. These bits have been delivered to Martin Marietta Corporation.

C. Three complete coring systems have been fabricated at L-DGO and will remain here for further testing.

RECOMMENDATIONS FOR FUTURE WORK

Accuracy of the HFE could be enhanced by improving thermal coupling between the drill stem and heat flow probes. Probes and drill stem with smaller diameter and lower thermal conductance would help to make these improvements. Coring operations presently planned do not make optimum use of the ALSD. Modifications to the ALSD including: use of the L-DGO coring system, changing the drill stem diameter, and lowering the drilling rate would improve the quality of the core, studies to determine the correct methods of deciphering a core obtained with rotary-percussive drills are required; lunar models of various geographic areas including those with stratified material should be cored experimentally.

APPLICATION OF A GLASS/BORON COMPOSITE
TO THE ALSD BIT EXTENSION

Phase I - Final Report

Prepared for

Lamont-Doherty Geological Observatory

Palisades, New York 10964

November 25, 1968

Submitted by

AVCO Government Products Group
Space Systems Division
Lowell Industrial Park
Lowell, Massachusetts 01851

1.0 INTRODUCTION

The program was divided into two separate consecutive phases. Phase I which is reported herein was a design and manufacturing feasibility study which was directed at proving the feasibility of using a boron/glass reinforced composite material for the Apollo Lunar Surface Drill (ALSD) bit extensions. The problems which were addressed in the program were

1. energy transmission
2. joint design
3. flute wear
4. thermal conductivity

The following paragraphs will discuss in detail each of these problem areas and describe the results of the work which was conducted in various tasks of the program.

2.0 ENERGY TRANSMISSION

From an evaluation of both the service requirements and fabrication limitations, a preliminary design concept was selected. This concept utilized a combination of boron and glass filaments. Uniaxial boron filaments were employed to obtain the highest possible axial stiffness and to eliminate the problems associated with wrapping boron at an angle. In fact, previous fabrication studies on this component eliminated wrapping boron at an angle of $22\frac{1}{2}$ degrees from the axis, an angle which would yield a highly desirable combination of axial and torsional stiffnesses. Because of this limitation, angle ply glass fiber were combined with the uniaxial boron to increase the torsional stiffness in addition to providing smooth,

non-splintering inner and outer surfaces. The non-splintering requirement becomes particularly acute at the tapered joints where it was hoped that the angle ply glass fiber would contain the boron so as to avoid flaring. One additional reason for the selection of glass in combination with boron was its low conductivity.

Several configurations of glass and boron were analyzed using the Avco Composites Analysis Program (2511). The predicted properties are given in the following table.

COMPOSITE PROPERTIES

| Boron Thickness (mils) | Glass Thickness (mils) | Axial Modulus (psi) | Shear Modulus (psi) |
|------------------------|---|---------------------|---------------------|
| 25 axial | 14 @ $\pm 45^\circ$ | 20×10^6 | 1.3×10^6 |
| 20 axial | 19 @ $\pm 45^\circ$ | 16×10^6 | 1.3×10^6 |
| 10 axial | 29 @ $\pm 45^\circ$ | 8×10^6 | 1.4×10^6 |
| 20 @ ± 10 | 19 @ $\pm 45^\circ$ | 15×10^6 | 1.7×10^6 |
| 15 axial | 14 @ $\pm 45^\circ$ 11 @ $\pm 8^\circ$ | 12×10^6 | 1.3×10^6 |

After investigating the thicknesses of glass filament that are commercially available, it was decided to select as a first attempt a configuration utilizing 7 mils of glass fibers wrapped at ± 45 degrees on both the inner and outer surfaces and 25 mils of boron sandwiched between. This combination would result in a total wall thickness of approximately 39 mils which is just short of the 40 mils required. This configuration yielded the following predicted mechanical properties:

$$\text{Axial Youngs Modulus} = 20 \times 10^6 \text{ psi}$$

$$\text{Torsional Shear Modulus} = 1.7 \times 10^6 \text{ psi}$$

Subsequent fabrication studies and the cost of very thin glass tape required that 14 mils of glass be used in the inner and outer layers with 15 mils of boron sandwiched between. The final configuration selected was the following

- a) 15 mils axial boron
- b) 14 mils @ $\pm 45^\circ$ glass for inner layers
- c) 11 mils @ $\pm 8^\circ$ glass for outer layers

The $\pm 8^\circ$ outer wrap was selected because of the 8° helix angle of the flutes. It was felt that this would ensure that glass filament would not be cut during the machining of the flutes and would improve the wear characteristics. The properties predicted for this configuration by program (2511) were the following

$$\text{Axial Young's Modulus} = 12 \times 10^6 \text{ psi}$$

$$\text{Shear Modulus} = 1.3 \times 10^6 \text{ psi}$$

Several tubes of this configuration were fabricated and cut into test samples for mechanical and thermal property measurements. The average mechanical properties measured were

$$\text{Axial Young's Modulus} = 11.6 \times 10^6 \text{ psi}$$

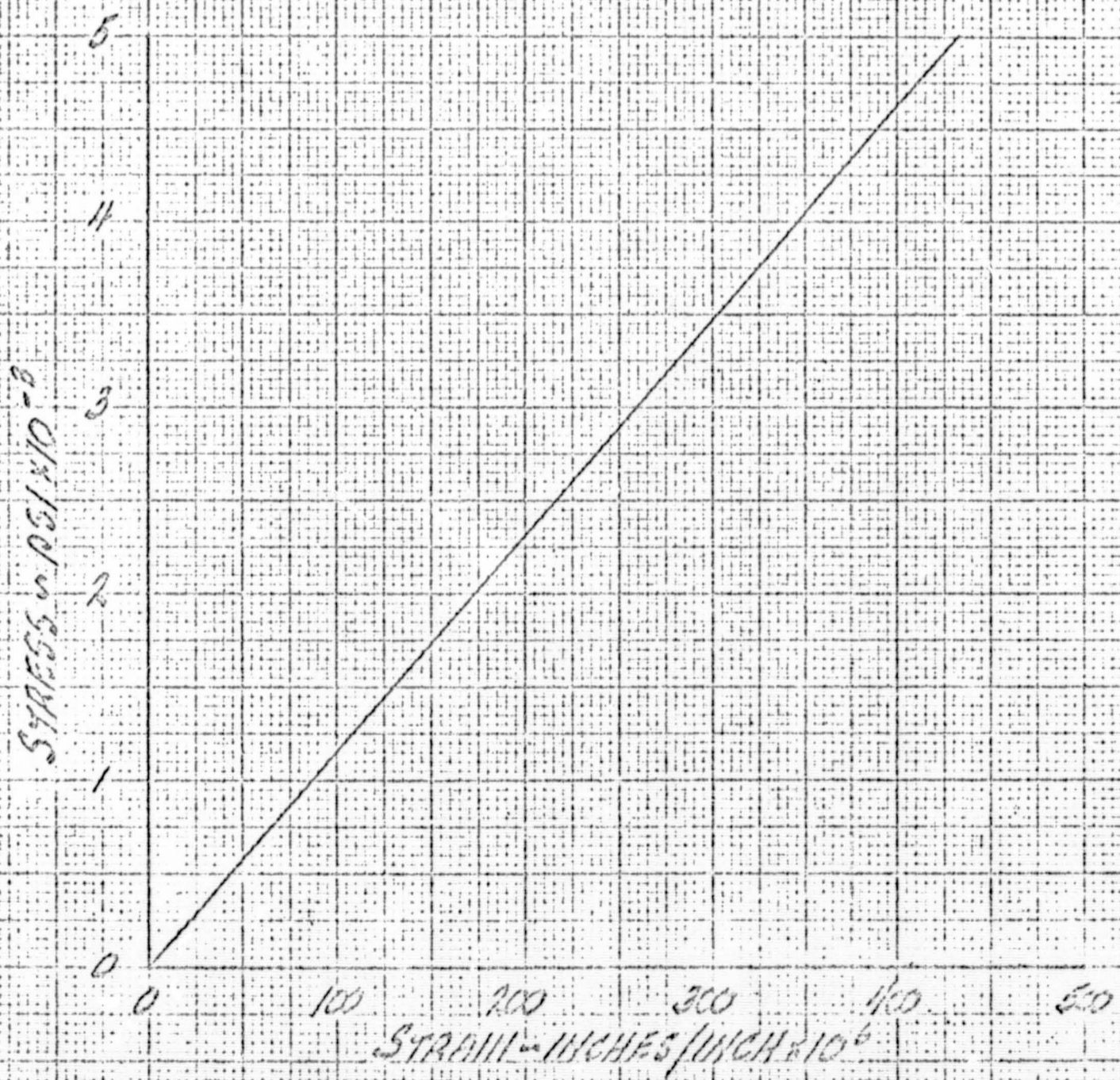
$$\text{Shear Modulus} = 1.57 \times 10^6 \text{ psi}$$

$$\text{Poisson's Ratio} = 0.20$$

A typical compressive stress strain curve for this configuration is given in figure 1.

REPRODUCIBILITY OF THE ORIGINAL PAGE IS POOR.

FIGURE 1
COMPRESSIVE STRESS STRAIN CURVE
FOR ALSD BIT EXTENSION MATERIAL



Several tubes of this configuration were tested in an actual drilling environment. None of the tests were successful as far as total operational requirements are concerned but from all indications it seemed that the energy transmission characteristics of the tubes were good. When it was possible to measure a drilling rate, the rate was comparable to that of the current titanium design. It is, therefore, possible to tentatively conclude that this configuration would provide adequate transmission of percussive energy in a drilling environment.

3.0 JOINT DESIGN

From the beginning of the program it was recognized by all concerned that success depended heavily upon developing a joint which would meet all of the design requirements. To expedite this development it was decided early in the program in conjunction with Lamont Geological Observatory to fabricate two full size bit extensions complete with flutes and provide a joint design similar to that shown in plan No. 38597, Hole Casing String Apollo Lunar Surface Drill, Martin Company, Martin Marietta Corporation. This was accomplished and the tubes were tested at the drilling test bed located at Martin in Baltimore. The test was a failure in that the joint failed immediately when drilling began. It was decided that this first attempt at fabricating a joint produced ^a joint of rather poor quality from both a fabrication and a machining standpoint.

A meeting was held the following week at Avco between Avco personnel and representatives of Lamont Geological Observatory. At that time it was decided to fabricate another joint of the same design making every effort to improve the fabrication quality and to provide more accurate and higher quality machining.

In addition, a new joint design was proposed by H. Gibbon of Lamont Geological Observatory in which the wall thickness constraint on the joint was relaxed thereby providing the possibility of increased strength in the joint area. This design is illustrated in figure 2. Although the design represented a very difficult machining effort, it was decided to fabricate a joint of this design for subsequent testing.

Both joint designs were fabricated, machined, and supplied to Lamont Geological Observatory for testing in simulated lunar surface test bed. The quality of these joints was superior to any that were previously fabricated and the machining of the joint was extremely precise.

The first joint, which was of the original design, failed during testing at Lamont Geological Observatory. Its performance, although superior to previous tests, was far from that which is required. An examination of the failure indicated that the boron had started to "broom" during the test. This phenomenon is similar to what occurs when two ~~brush~~ brushes are pushed together. To correct this, H. Gibbon of Lamont Geological Observatory suggested that a metal insert be incorporated in the design so that the energy would then be transmitted from the boron in one tube through smooth metal surfaces to the boron in the other tube. It was decided to incorporate this idea in the second joint design. The metal insert is illustrated in the joint drawing (figure 2). The new joint design was subsequently tested and failed. This failure indicated a lack of axial strength in the outer layers of glass.

At this point all possible alternatives had been attempted to date within the allotted funds without obtaining a successful joint. Further joint development would have to be funded either by money which had been allotted to phase II or from a new source.

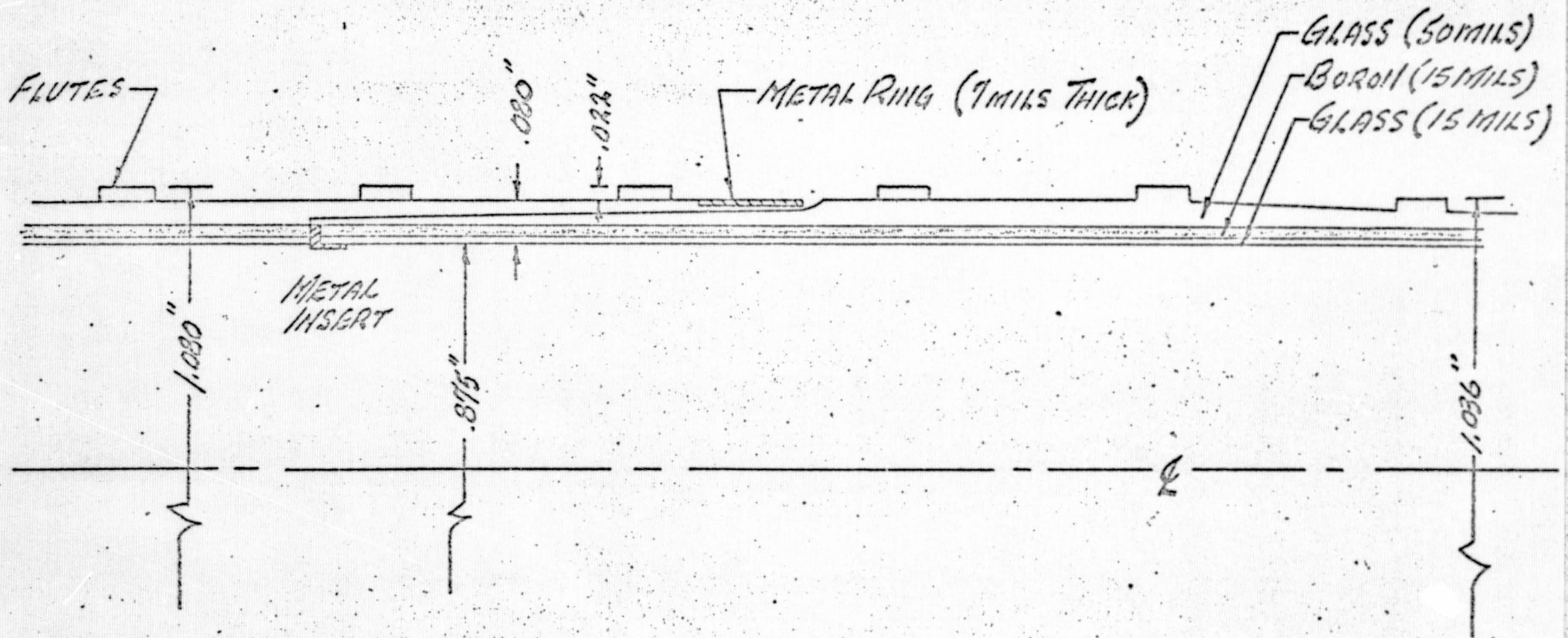


FIGURE 2 TAPERED JOINT (DESIGN #2)

Avco suggested that any future joint development work in the program should include the use of a glass fabric for the outer layer of the tube. This was prompted by the fact that the existing casing tubes are fabricated from glass fabric and have never exhibited failures of the type which have been experienced thus far in the program.

Lamont Geological Observatory suggested that Avco seek the assistance of Mr. Wilson of Arthur D. Little Co. who is an expert in advanced filament winding techniques. The basis for this suggestion was the feeling that the problem with the joint failures stemmed from filament winding techniques and a resulting part of poor quality. Avco did not agree with this viewpoint since the tubes fabricated by Avco had mechanical properties at least as high and often higher than those predicted analytically. This difference of opinion will never be solved satisfactorily, however, since Mr. Wilson proposes to fabricate tubes with outer wraps whose orientation will produce mechanical properties similar to those obtainable from glass fabrics which Avco had proposed.

In a final attempt to maintain the integrity and continuity of the program Avco proposed that limited funds be made available to Mr. Wilson for fabricating a joint of his design. The cost for this effort would be absorbed by phase II funding, but if Mr. Wilson was successful, Avco would complete Phase II of the program for the original negotiated sum minus the amount required for Mr. Wilson's effort. This proposal was unacceptable to Lamont Geological Observatory who decided to fund Mr. Wilson independently from funds which were available for Phase II and to cancel Phase II funding to Avco.

In conclusion it can be stated that the joint problem has not been solved at this time. A myriad of suggestions can always be offered which might prove the feasibility of the concept, but available funding will severely limit the number of these approaches that can be attempted.

4.0 FLUTE WEAR

The wear characteristics and the design of a flute fabricated from a fiber reinforced plastic was of prime concern at the inception of the program. Early in the program it was decided that the existing flute design was the most feasible from a fabrication standpoint and attention was directed at finding ways to improve the wear characteristics of the flute.

To accomplish this Avco proposed that various additives be incorporated with the resin utilized in the design. The additives considered were

- a) graphite powder
- b) teflon
- c) chopped silica

These tests were intended to give a qualitative assessment of the effects that these additives would have on the wear characteristics of the tubes.

The test specimens were fabricated as shown in figure 3.

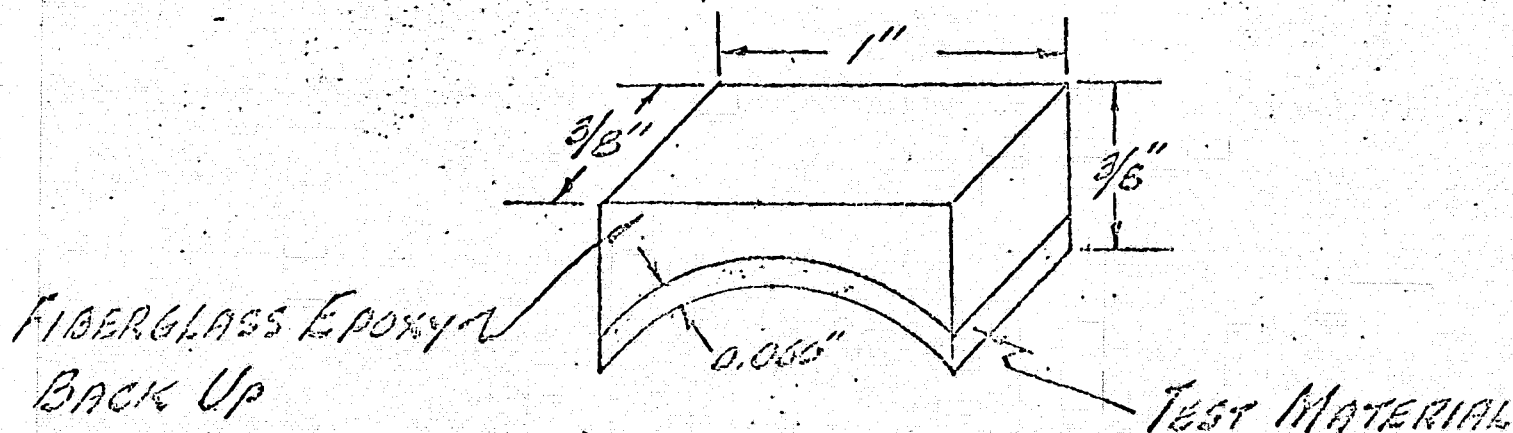


FIGURE 3 WEAR TEST SPECIMEN

The tests were conducted in an Avco wear tester which incorporated an abrasive wheel which rotated with little or no normal force against the curved face of the test specimens. The wear of a particular sample was assessed by measuring the amount of test material removed from a given sample after travelling a given peripheral distance. The results of these tests are given in the following table.

WEAR TEST RESULTS

| Additive | Wear after travelling 1000 ft | Wear after travelling 11,000 ft |
|-----------------|-------------------------------|---------------------------------|
| graphite powder | .013" | Worn through |
| teflon | .003 | .027 |
| chopped silica | .004 | .019 |
| None | .010 | Worn through |

It is apparent from the table that both teflon and chopped silica provided improved wear characteristics for the tubes and both should be assessed in any future development programs.

5.0 THERMAL CONDUCTIVITY

The thermal conductivity of the final configuration of the ALSD bit extensions was of prime importance throughout the entire program since the success or failure of the entire experiment depended heavily upon keeping this property

at a low level. Samples of the final tube configuration described in section 2.0 (3 layers of boron) were submitted to Avco's Thermal and Chemical Properties Section for evaluation. Figure 4 gives the thermal conductivity as measured axially in a vacuum for the test specimens. The values of conductivity obtained are in the range of ceramics. They are higher than optimum but acceptable for the current program.

FIGURE 1-

THERMAL CONDUCTIVITY VS TEMPERATURE

THERMAL CONDUCTIVITY W/WT%

$P = 115.7 \text{ LB/FT}^3$
TEST DATE: 25 SEPT 1969
CONDUCTIVITY MEASURED
AXIALLY IN VACUUM (Pressure
100 MICRONS)

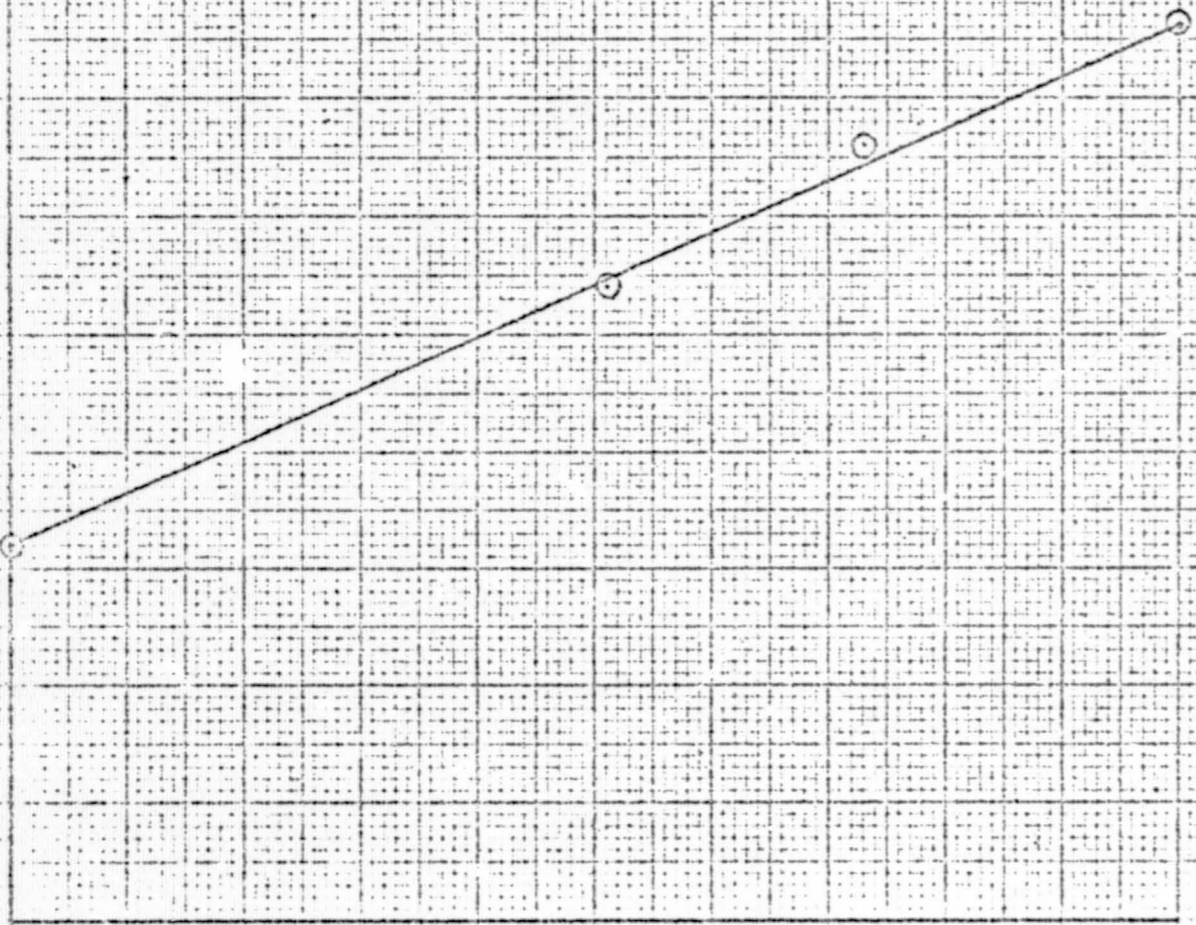
11
10
9
8
7
6
5
4
3
2
1
0

100

200

300

TEMPERATURE °F



REPRODUCIBILITY OF THE ORIGINAL PAGE IS POOR.

THERMAL CONDUCTIVITY MEASUREMENTS OF BORON-REINFORCED FIBERGLASS TUBEI. INTRODUCTION

The ALSEP Heat Flow Experiment will use two heat flow probes each emplaced in a 3 meter borehole in the lunar surface. The borehole will be cased with a boron-reinforced filament-wound fiberglass tube used as the drill stem. The temperature gradient and thermal conductivity measurements made by the heat flow probes are influenced by the thermal properties of the borehole casing. To provide data needed in estimating the effects of the casing on the probe's measurements, we measured the thermal conductivity of a typical section of the borehole casing.

II. METHOD AND APPARATUS

The longitudinal heat flow method was used to evaluate the thermal conductivity of a prototype section of boron-reinforced fiberglass tube, 15 1/2 inches long. After carefully measuring the tube dimensions, fourteen 0.003" diameter chromel-constantan thermocouples were cemented in small holes drilled into the tube. Most of the thermocouples were located in the boron layer of the tube; others were located in the outer fiberglass layer. A 1000 ohm wire wound resistance heater was placed inside the tube at its midpoint and cemented to the tube with Dow Corning 340 epoxy. Copper end plugs, with cooling coils, were fixed to each end of the tube. The void space within the tube was filled with open cell urethane foam of approximately 2 lb/ft³ density. The foam conductance is very much lower than that of the sample and can be neglected. The outside surface of the tube was insulated with approximately 12 layers of multi-layer insulation -- each containing an aluminized mylar shield and a woven fiberglass cloth spacer. The insulation was applied in a continuous wrap; the thermocouple wires were led out from the casing sample tube within the insulation. A schematic diagram of the apparatus is shown in Figure 1.

The boron-reinforced tube, together with thermocouples, end plugs, heater and insulation were placed on a laboratory vacuum table and covered with a bell jar. The assembly was evacuated to 10⁻⁵ Torr or less. A constant temperature fluid was circulated through the coils of the end plugs; electric power was applied to the heater using a controlled dc power supply. An experimental measurement consisted of: 1) providing a controlled temperature fluid in the end plugs; 2) applying a constant electric power to the heater; 3) waiting a sufficient period (8-24 hrs) for a steady state temperature distribution to be established in the tube; 4) recording the thermocouple emfs (using a L&N type K-3 potentiometer and null meter) and the heater current and voltage. Measurements were made at three temperature levels: room temperature, 230°K and 330°K. Temperature measurements were accurate to about ± .25°C. Several heater power levels were used. During the measurements program, when it was determined that radial heat losses were extensive, an additional layer of fiberglass insulation, approximately 1/2" thick, was added to the outside of the already insulated bore tube.

III. RESULTS AND DISCUSSION

The original concept of the measurements required that the radial heat interchange between the tube and its surroundings be small so that one dimensional heat flow in the bore tube would result. Under these conditions, the temperature distribution in the tube should be linear and the conductance of the tube (the conductivity-area product) could be evaluated from the heater power and slope of the temperature - distance curve. Because of the low conductance of the tube, its relatively high surface area, and the low insulating effectiveness of the insulation applied to the tube, radial heat flow was significant in almost all tests and an alternate method of analysis had to be adopted.

Figure 2 shows typical temperature profiles for several tests at room temperature. Note the linearity for tests 6 and 23 and the curvature for test 5. High and low temperature test data are shown in Figures 4 and 5. For these tests, the large radial heat flow made it difficult, if not impossible, to derive reliable values of conductance at low and high temperatures; however from tests at room temperature, particularly those where several power levels were used, reliable values of conductance can be determined.

A. Room Temperature Results

Test runs 6, 7, 14, 19 and 23 were conducted at room temperature with a relatively low power applied to the heater. Because of the small difference between the temperature of the bore tube and the surroundings, radiation losses were small and the temperature gradient along the tube was almost linear. If we assume negligible heat losses, the conductivity-area product can be calculated from the equation:

$$kA_x = \frac{q}{\Delta T/L} \quad (1)$$

where q is half of the electric power applied to the heater (one half flows in each direction), and $\Delta T/L$ is the temperature gradient. The results are shown below:

| <u>Test</u> | <u>Heater Power</u> (watt) | <u>Average Temperature</u> (°K) | <u>kA_x</u> (watt cm/°K) |
|-------------|-------------------------------|------------------------------------|--|
| 6 | .0079 | 300 | 0.012 |
| 7 | .0075 | 300 | 0.012 |
| 14 | .0031 | 296 | 0.013 |
| 19 | .0077 | 299 | 0.015 |
| 23 | .0079 | 301 | 0.013 |

and indicate that the conductance is probably 0.013 ± 0.001 watt cm/°K.

However, careful examination of the temperature-distance plots show some curvature, particularly for those tests at higher heater power and at locations near the center of the tube. This is expected if heat is lost from the tube to the surroundings.

As an alternate method of evaluating conductance, we assumed that the heat losses were proportional to the difference between the average tube temperature, T_m , and the ambient temperature, T_o . Then the electrical power dissipation can be related to the losses and the heat flow in the tube as follows:

$$q_h = \frac{kA_x}{L} (T_1 - T_2) + h\pi DL (T_m - T_o) \quad (2)$$

where T_1 and T_2 are the heater temperature and heat sink temperature, D is the tube diameter, L the tube length between the heater and the heat sink, and h is the heat transfer coefficient. Equation 2 can be rearranged as follows:

$$\frac{q_h}{(T_m - T_o)} = \frac{kA_x (T_1 - T_2)}{L (T_m - T_o)} + h\pi DL \quad (3)$$

For an almost linear gradient in the tube $T_m \approx \frac{T_1 + T_2}{2}$.

A plot of $q_h / (T_m - T_o)$ versus $(T_1 - T_2) / (T_m - T_o)$ should give a straight line of slope kA_x / L and intercept $h\pi DL$, thus providing a means for estimating kA_x / L and h . Figure 3 shows such a plot for the room temperature data, including the points where losses may be significant. In drawing the line through the data, the results of test 17 were weighted only slightly because of the small temperature drop along the tube (0.45°C) and small difference between the ambient temperature and the tube temperature. Similarly, in test 5, the data point was discounted since the heat losses were the greatest and the temperature-distance curve was decidedly nonlinear. From the slope of the plot of all other data points from tests at about 300°K , the value of kA_x is found to be approximately 0.011 watt $\text{cm}/^\circ\text{K}$ -- slightly lower than that assuming no heat losses. From the intercept, we find that $h = 2.1 \times 10^{-6}$ watt/ $\text{cm}^2 \cdot ^\circ\text{K}$.

The radiation heat losses during the tests can also be estimated using an analytical model where a cylindrical fin of length L has its ends held at temperatures T_1 and T_2 and is radiating to surroundings at T_o . The temperature distribution in the tube is:

$$T - T_o = \frac{(T_1 - T_o) \sinh m(L-x) + (T_2 - T_o) \sinh mx}{\sinh(mL)} \quad (3)$$

where T_1 and T_2 are the temperatures at $x=0$ and at $x=L$, respectively.

By matching theoretical and experimental temperature profiles, the value of m can be estimated, where:

$$mL = \sqrt{\frac{h\pi D}{kA_x}} L \quad (4)$$

$$h = \frac{kA}{\pi D} \left(\frac{mL}{L} \right)^2 \approx 4\sigma F_e F_A T^3 \quad (5)$$

In Figure 2, theoretical curves are shown for $mL = 1.0$ and $mL = 1.2$. The best match is obtained at about $mL = 1.3$ which corresponds to a value of

$$h = \frac{(.011)}{\pi(2.5)} \left(\frac{1.3}{17.1} \right)^2 = 8 \times 10^{-6} \text{ watt/cm}^2\text{K} \quad (6)$$

This test was conducted before the 1/2" fiberglass insulation was installed and represents the effect of 12 wraps of multilayer insulation. The equivalent emittance factor would have a value of $F_e \approx .013$. The theoretical factor for 12 ideal wraps having an emissivity of .025 per surface would be about .001. The actual insulation performance is less good than anticipated, although the ideal value could not be achieved in practice because of effects such as 1) the conductance through the spacer 2) the spiral wrap (instead of floating concentric shields) 3) presence of thermocouple leads 4) slightly tight wrap.

Tests following #16 were run with additional insulation installed outside the multilayers. One might expect to see in Figure 3 a displacement between data from tests 5, 6, 7, 14 and from tests 17, 19, 23 which would indicate different values of the intercept or equivalent loss coefficient, h . Test 5 may reflect this effect. However, tests 6, 7 and 14 all had "cold end" temperatures below room temperature so that heat could be lost to the surroundings near the warm end and gained near the cold end. Net losses would be small for these tests and would not give a realistic estimate of h . Close examination of the temperature profile for Test 6 (figure 2) shows this effect since the data actually indicate an S-shaped curve around the straight line drawn. The slope decreases slightly with distance from the heater at the warm end indicating a heat loss. The opposite effect can be detected near the cold end.

B. High Temperature Results

Data at about 330°K were obtained by controlling end temperatures at about 65°C. Data from a typical test are shown in Figure 4. This test was conducted at a high power level and the shape of the curve is indicative of substantial heat losses. In earlier tests with no power and with low power, the heater temperature was actually lower than the controlled end temperatures since the system was losing heat to surroundings at about 22°K.

The same fin model described in the previous section (equation 3) again is applicable and allows an estimate of losses to be made using eqs. 4 and 5. For test 51 shown in Figure 4 and for the $q = 0$ test, the best match was obtained using $mL = 0.6$. This corresponds to

$$h = \frac{.011}{\pi(2.5)} \frac{0.6^2}{17.1} = 1.7 \times 10^{-6} \frac{\text{watts}}{\text{cm}^2 \text{ } ^\circ\text{K}} \quad (7)$$

or

$$F_e = \frac{1.7 \times 10^{-6}}{4(5.67 \times 10^{-12})} (350)^3 = .002 \quad (8)$$

This is for the system after addition of fiberglass insulation over the multilayer wrap. The magnitude of this value seems reasonable and is in agreement with the value of h obtained from the intercept of Figure 3.

C. Low Temperature Results

Figure 5 presents the temperature profile for a typical low temperature test. In these tests, the coolant temperature was controlled at about -65°C . Since the surroundings were at about 22°C , in these tests heat was flowing through the insulation into the test section. The shape of the profile in Figure 5 shows this effect.

The fin analysis indicates that $mL \approx 0.7$ for the low temperature tests. The equivalent value of h is about 2.3×10^{-6} watts/cm²°K. This represents radiation from about a 300°K temperature level and would result in an estimate of $F_e \approx .004$. However, since the outer insulation is now the heat source^{a, e}, the effective area factor F_a is likely to be greater than unity.

IV. CONCLUSIONS

1. The measured conductance of the boron-reinforced epoxy - fiberglass casing at 300°K is about 0.011 watt cm/°K. This value has an accuracy of about $\pm 10\%$.

2. Tests at 230°K and 330°K temperature levels give results consistent with the room temperature tube conductance and reasonable losses or gains of heat through the sample insulation. These results are not sufficiently accurate to allow an experimental determination of the conductance variation with temperature level.

3. Previous predictions for casing conductance based on geometry and literature values for boron, tungsten and epoxy-fiberglass indicated values of $kA = .025$ watt cm/°K at 200°K and $= .020$ watt cm/°K at 300°K . The difference in predicted and measured conductances probably is due to uncertainty in the conductance of the boron fibers which represent 75% of the casing conductance. No data for boron fibers were located, so literature values for boron crystals (1) were used in the calculations. Deviation from a pure crystalline form would lower conductance, therefore the measured values are consistent with expectations based on the predicted values. The 10% decrease in conductance between

200°K and 300°K reported in the literature is probably applicable to the experimental data.

V. RECOMMENDATIONS

The following values should be used as axial thermal conductances for the HFE drill casing:

$$kA_x = .011 \pm .001 \text{ watt cm/}^\circ\text{K at } 300^\circ\text{K}$$

$$kA_x = .012 \pm .002 \text{ watt cm/}^\circ\text{K at } 200^\circ\text{K}$$

(1) Thompson, J.C. and W. J. McDonald, "Low Temperature Thermal Conductivity of Boron" in Gavle, "Boron," Vol. 2 Plenum (1965)

REPRODUCIBILITY OF THE ORIGINAL PAGE IS POOR.

BY..... DATE.....
APPROVED..... DATE.....
CLIENT.....

ARTHUR D. LITTLE, INC.
CAMBRIDGE, MASS.

SHEET NO..... OF.....
SKETCH NO.....
CASE NO.....

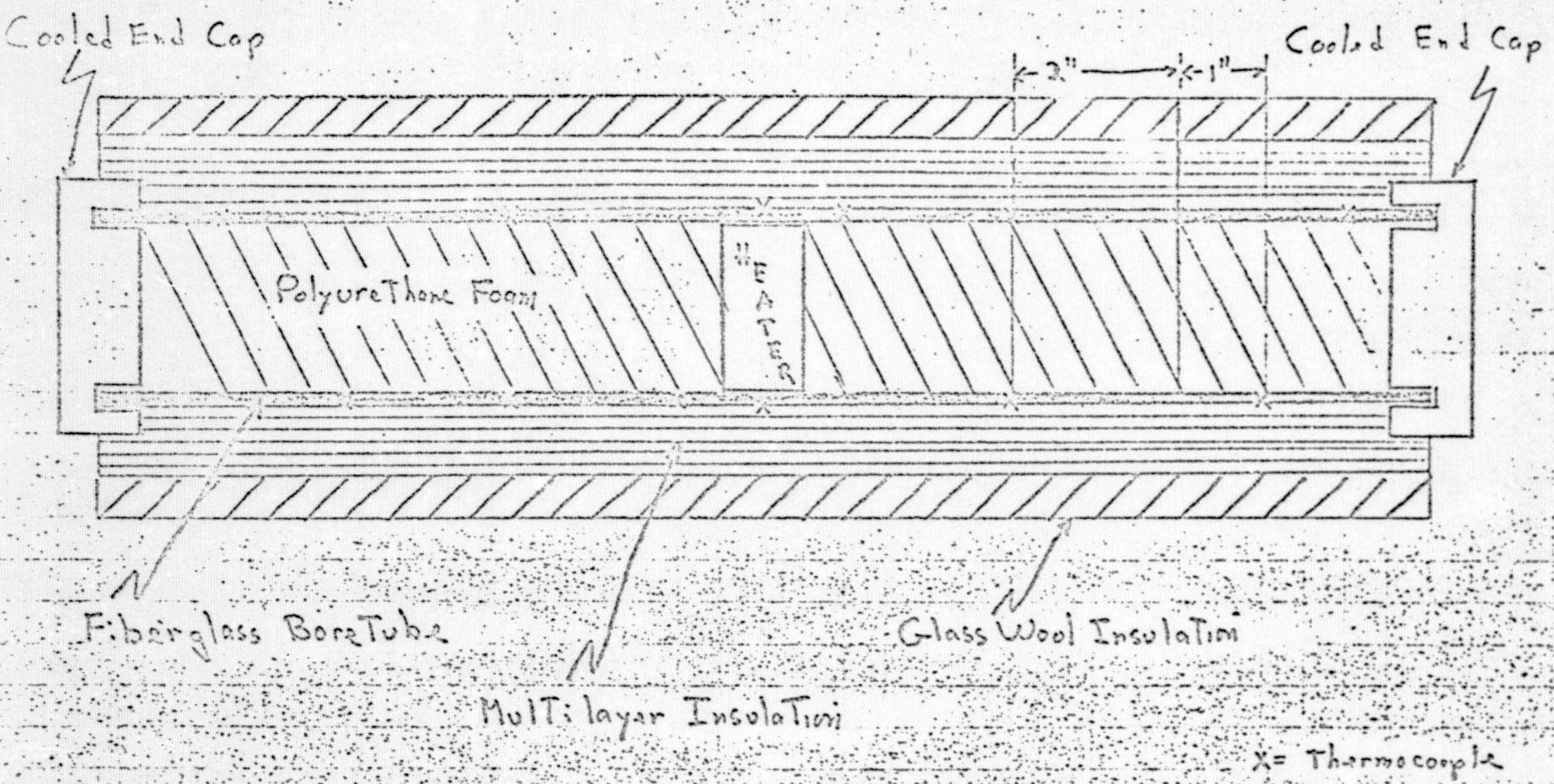
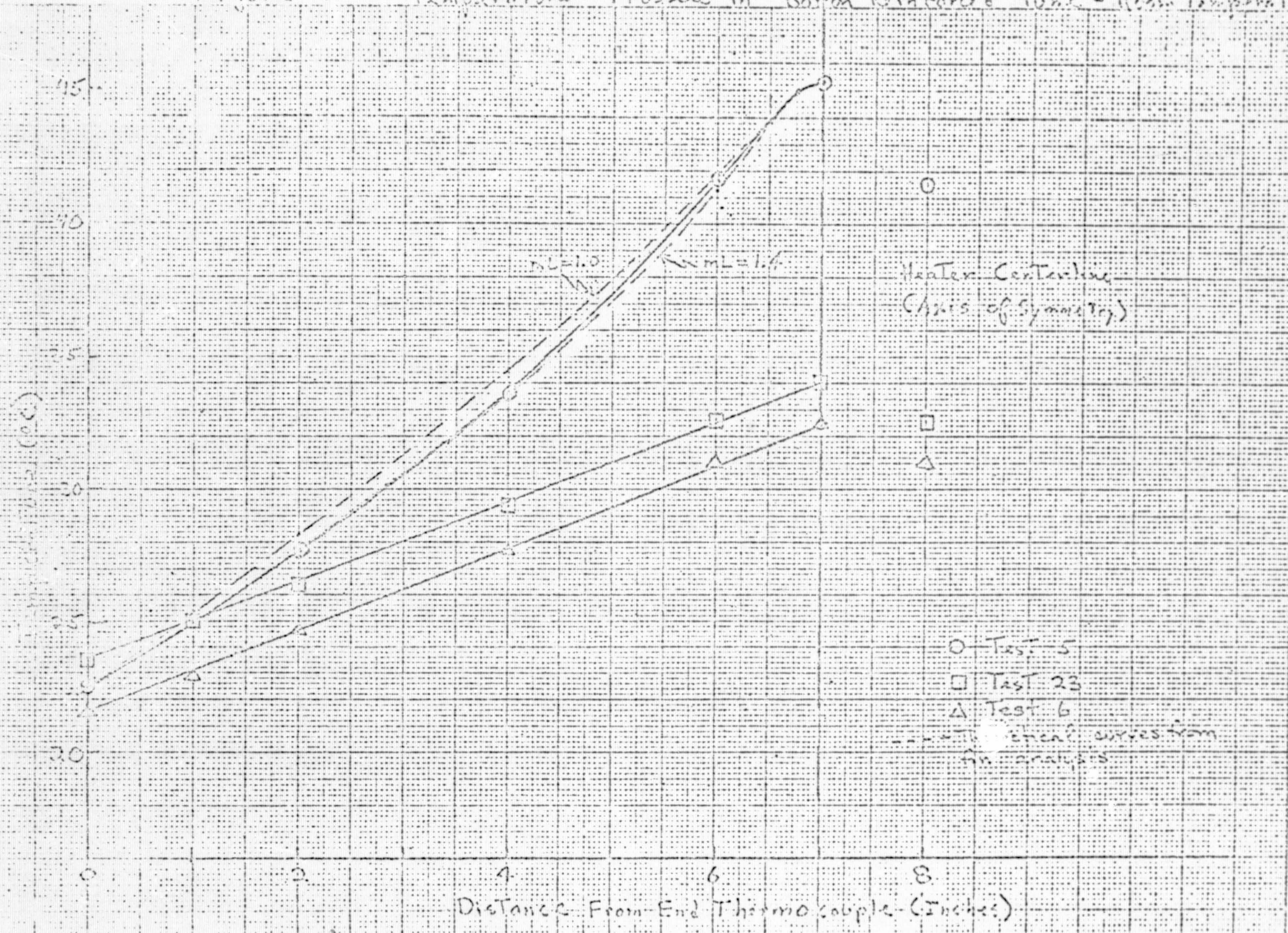


Figure 1 Schematic Diagram of Apparatus

Figure 2 Temperature Profile in Boston Reinforced Tube - Room Temperature



REPRODUCIBILITY OF THE ORIGINAL PAGE IS POOR.

Fig 3.
Estimate of Casing Conductance
From Room Temperature Data.

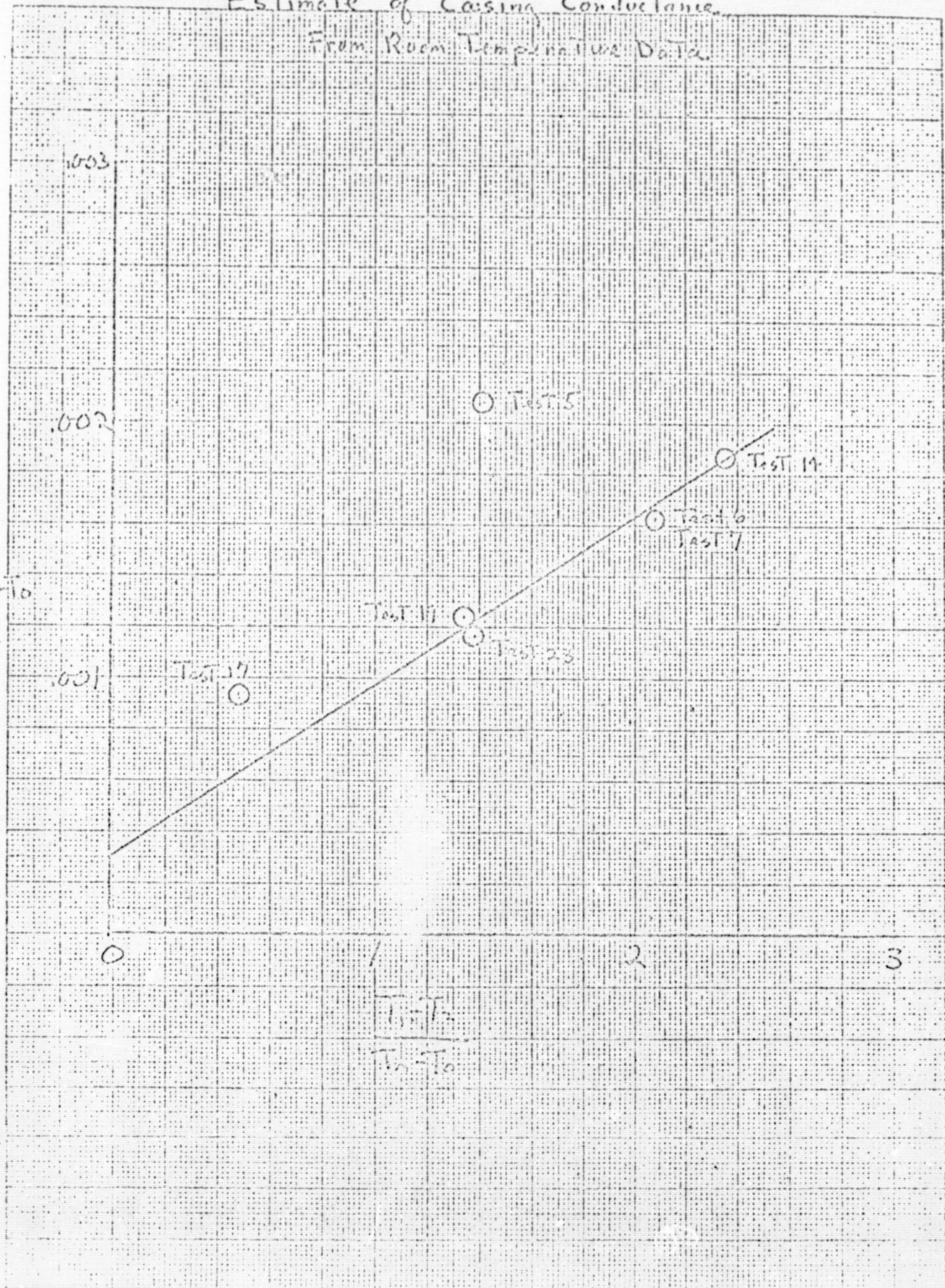
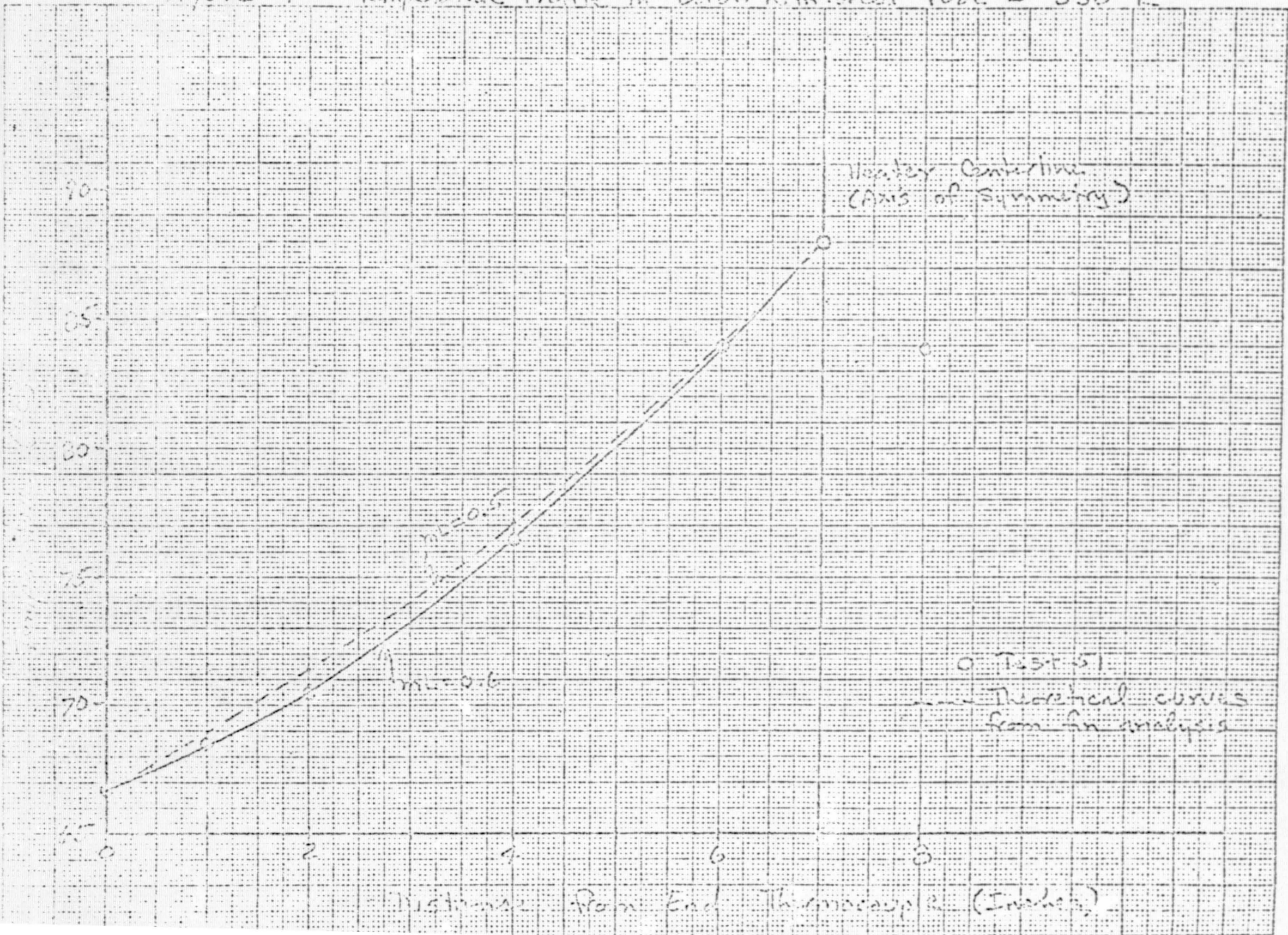
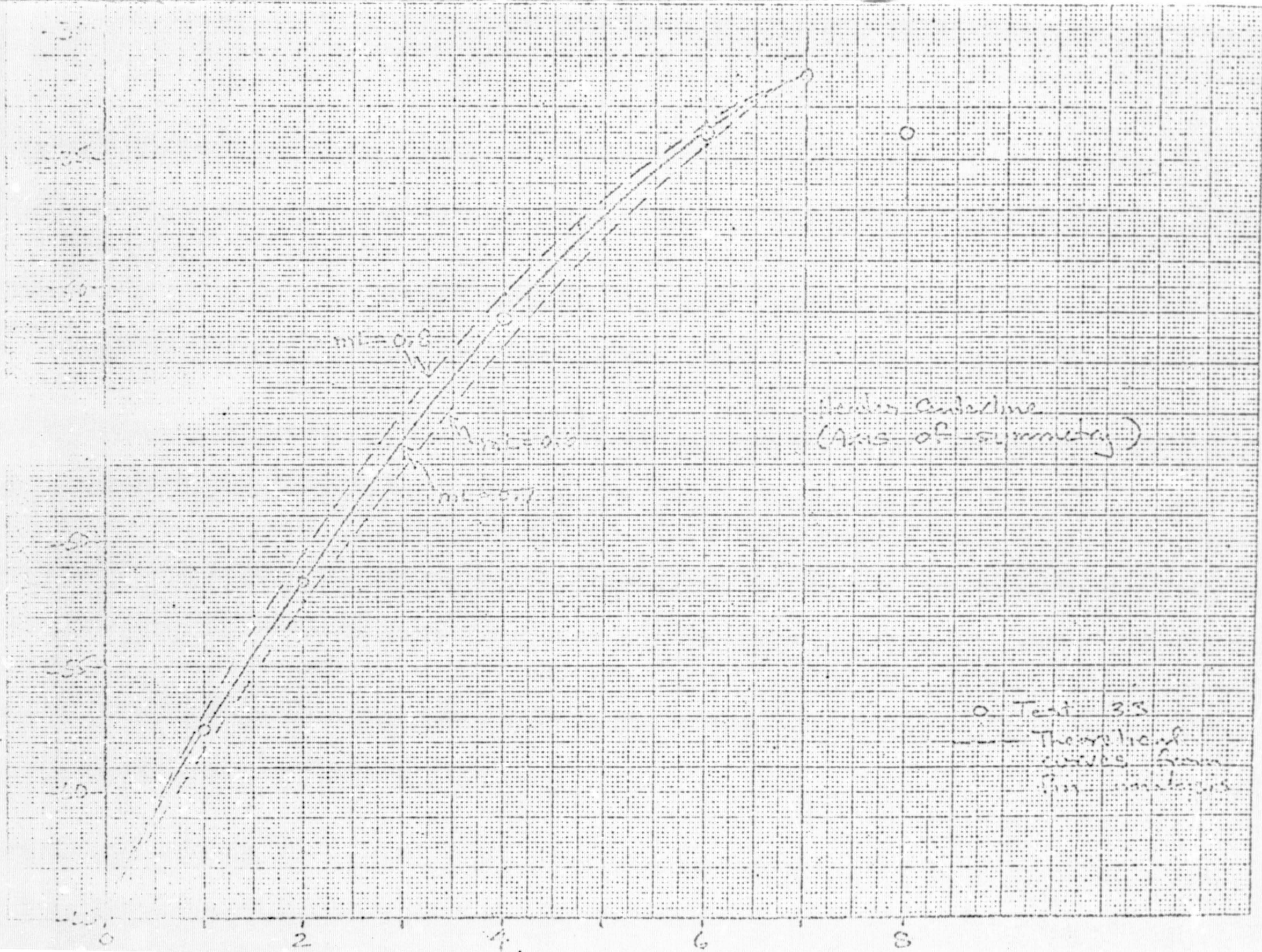


Figure 4 Temperature Profile in Boron Reinforced Tube - 330 °K



REPRODUCIBILITY OF THE ORIGINAL PAGE IS POOR.



REPRODUCIBILITY OF THE ORIGINAL PAGE IS POOR.

PRELIMINARY REPORT

Drill Tests During January

at Lamont-Doherty Geological Observatory
of Columbia University
Palisades, New York

-o-

M. G. Langseth

Richard Perry

-o-

This work is being done under a
supplementary agreement to NAS 9-6037

January 26, 1969

SUMMARY OF TESTING AT LAMONT IN JANUARY

Purpose:

1. Test the new taper joint fabricated by ADL.
2. Determine the drilling rate with the solid-faced bit using three types of drill stem: titanium, boron reinforced fiber glass, fiber glass with axial glass core.
3. Determine drilling rate using the new 1 $\frac{1}{4}$ " diameter bit.

Procedure:

Test of taper joint:

1. Run the new taper joint for a short period in the barrel of basalt dust. Run drilling tests in the dense basalt block for a total of about five minutes. Then run drilling tests in vesicular basalt for five minutes.

Equipment:

Black and Decker rotary percussive drill model #723. Lamont drill test facility, ADL boron reinforced epoxy fiber glass taper joint Model #2, ADL boron reinforced epoxy fiber glass drill stem; two joined 20" sections, ADL fiberglass tube axially reinforced with glass fibers, ALSD titanium drill string. Four types of Chicago-Latrobe drill bits: the 1.027" diameter solid-faced bit (Lamont modification), the 1.027" diameter coring bit (flight configuration), 1.125" diameter coring bit, and 1.250" diameter coring bit.

Description of tests:

Test of new taper joint

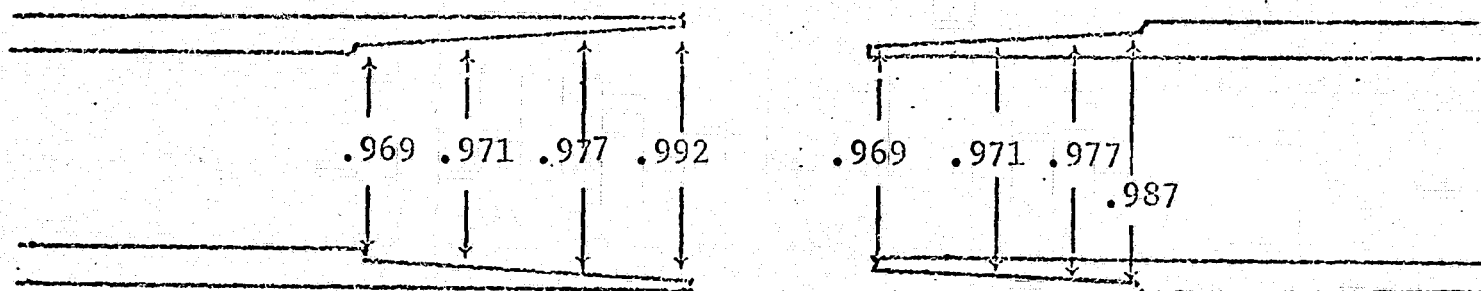
| Test Number | Test Material | Type Bit | Type Stem | Drilling Time | Penetration | |
|-------------|---------------|-------------|-------------------|---------------|-------------|-------|
| | | | | | Start | End |
| 1 | Basalt Dust | Core 1.125" | Boron Taper Joint | 15" | | |

Remarks:

At the start of drilling the top of the female joint began to discolor immediately and a fine yellowish-white powder formed in front of the steel reinforcing ring on the female joint. After drilling down once, the joint was slipping freely and was very hot.

Diagnosis:

Precise measurements were made of both the male and female joint. with the results shown below.



From the measurements it is clear that the two tapers are a snug fit when mated up. Initially however the male should be .004" larger on the diameter point for point so that radial stresses are built up when the two joints are firmly mated together. It appears however that one of the joints had given so that this interference was lost. Later tests showed this expansion was probably in the female.

January 24th we tried to bring the female back down to size by means of brass hose clamps. However these hose clamps easily shook loose when percussion started. Tests with hose clamps yielded results similar to those on the preceding day.

Tests of drilling rate:

TABLE 1: Results of drilling rate tests January 23 & 24, 1969.

| Test Number | Bit | Stem | Penetration | | Drilling Rate |
|-------------|----------------|----------------|-------------|-------|---------------|
| | | | Start | Stop | |
| 1 | Solid 1.027 | Boron | 0.211 | 1.248 | 1.037 in/min. |
| 2 | Solid 1.027 | Boron | 1.248 | 2.239 | 0.991 in/min. |
| 3 | Solid 1.027 | Fiber Glass | 2.239 | 3.156 | 0.817 in/min. |
| 4 | Solid 1.027 | Fiber Glass | 3.156 | 3.971 | 0.815 in/min. |
| 5 | Solid 1.027 | Boron | 3.971 | 4.944 | 0.973 in/min. |
| 6 | Core 1.250 | Boron | 0.161 | 0.480 | 0.319 in/min. |
| 7 | Core 1.250 | Fiber Glass | 0.480 | 0.744 | 0.264 in/min. |
| 8* | Core 1.250 | Titanium | 0.744 | 1.051 | 0.460 in/min. |
| 11 | Core 1.027 | Fiber Glass | 0.066 | 0.593 | 0.527 in/min. |
| 12 | Core 1.125 | Fiber Glass | 0.978 | 1.422 | 0.444 in/min. |
| 13 | Solid 1.027 | Titanium | 0.601 | 1.445 | 0.844 in/min. |

* The flutes, which also have a diameter of about 1.250, jammed on walls of hole. This can be cured by cutting down flutes.

Test material was dense basalt. The duration of all drill tests was one minute except for test 8 which was 40 seconds.

Discussion:

Taper joint: The cause of the failure of the taper joint was the loss of the interference fit when the joint made up. This appeared to result from the expansion of the tapered female sleeve. Secondary effect was the actual grinding away of material on both taper surfaces when they rotated relative to one another. However this grinding would not have occurred had the female sleeve not expanded.

This is the first time in the development of the taper joint that we have had slippage due to torque once the joints were mated. In my opinion this was due to intrinsic weakness in the female sleeve. The glass filaments are interwoven at 45° to the axis. This weave does not have very high circumferential strength thus allowing the sleeve to expand under quite low radial stresses.

Secondly, the inside taper of the female sleeve has been relieved where it joins the body of the stem so that when the joint mated, all of the strain was taken up in the sleeve alone. Earlier the tapers were straight and some of the radial strain had to be taken up by the body of the drill stem beyond the taper. In addition this model of the taper joint had very strong steel reinforcing ring inserts which prevented the stem from giving radially. These difficulties can be overcome by:

1. Strengthening the female taper sleeve by a circumferential wrap of glass fibers.
2. Return to the straight taper so that the body of the stem helps take

up the strain when the joint is mated.

3. Remove the steel reinforcing rings to increase the radial yield of the stem on both the male and female.

Removing the steel reinforcing rings results in a secondary problem. Some cladding must be provided to end off the boron filaments to prevent them from delaminating under the stresses of drilling. The drilling performance of the fiber glass (see the results of the drilling rate tests) suggests that if we end off boron filaments with circumferential glass filaments there is little loss in the percussive energy.

The removal of the steel reinforcing rings will greatly improve the thermal performance of the drill stem, since it will have a uniformly low conductivity along its length.

Discussion of the drilling rate tests:

To make drilling rate comparison tests we used a block of very dense basalt. This rock is quite uniform in hardness and texture throughout and numerous tests show that quite repeatable drilling rates are obtained in different parts of the rock slab. The test results presented earlier and the results of tests taken the first week in January are given in matrix form below. Primarily we vary the drill stem material. With each type of drill stem we used four different bit configurations and sizes.

Table of drilling rate in in/min.

| Type of Drill Bit Type of Stem | 1.027 Kerf Solid Area (0.821) | 1.027 Kerf Core Area (0.391) | 1.125 Kerf Core Area (0.558) | 1.250 Kerf Core Area (0.789) |
|-----------------------------------|-------------------------------------|------------------------------------|------------------------------------|------------------------------------|
| Fiber Glass | 0.82 (2) | 0.53 (1) | 0.44 (1) | 0.26 (1) |
| Boron | 0.99 (2) | 1.20 (1) | 0.71 (2) | 0.32 (1) |
| Titanium | 0.84 (1) | 1.10 (1) | 0.65 (1) | 0.46 (1)* |

All tests were made in dense basalt.

*All tests are based on drilling one minute except that marked with an asterisk which lasted 40 seconds.

Number in parentheses gives number of tests averaged.

The solid-faced versus the core bit:

The low rate when using fiber glass stem and a core bit 1.027" in diameter is thought to be atypical. The results of comparing the two types of bits with the boron and titanium are probably more valid. These results indicate that the energy required to break up the core reduces the drilling rate about 15 to 20%. This reduction is certainly not in proportion to the volume of rock being removed. Thus a solid-faced bit can be used on the ALSD with very little reduction in the reliability.

Comparison of bit sizes:

Comparison of columns 2, 3 and 4 summarized in Figure 1 show a reduction in drilling rate with kerf area.

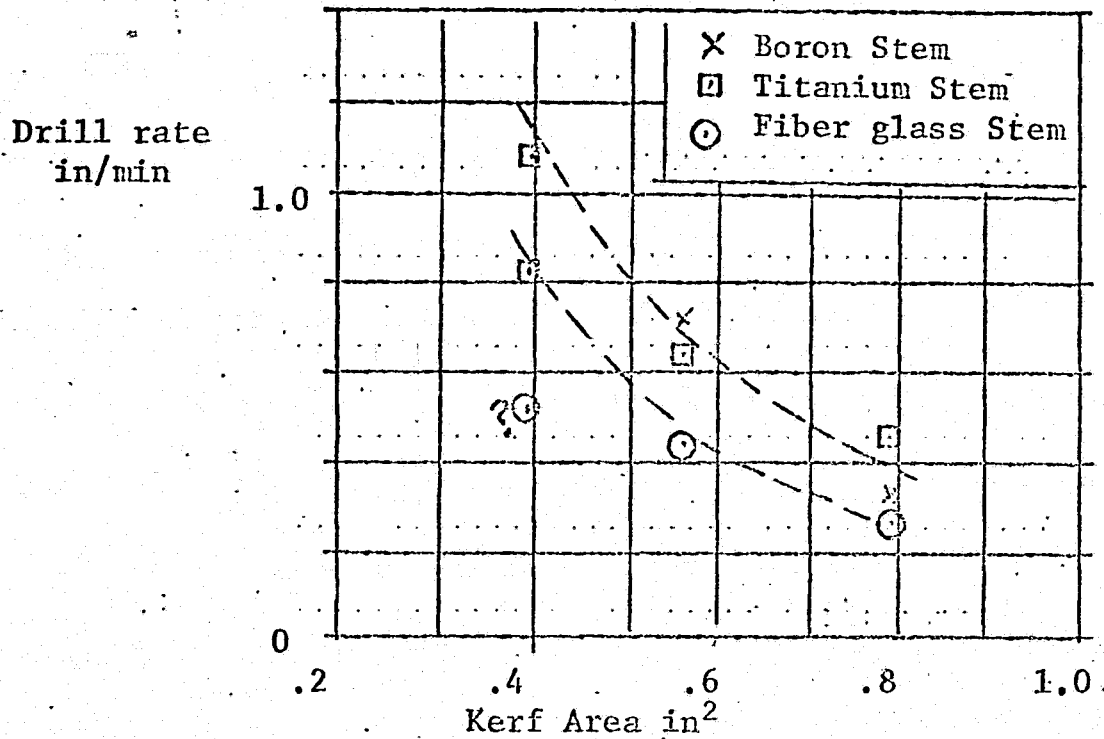


Figure 1. Drilling rate versus kerf in dense basalt.

To a first approximation it falls off in proportion to the kerf area. This plot clearly shows the great advantage of Lamont solid-faced bit design.

One very important consequence of these tests is to show that the kerf area must be kept to a minimum. In making a solid-faced bit 1.125" in diameter it is desirable to keep a kerf width of .141. Thus the kerf area would be 0.436 and we can predict a drilling rate of a core type bit of about 1.0 in/min with titanium or boron stem. With addition of a core breaker the rate would probably be lower to about 0.80 to 0.85 in/min.

Comparison of different types of drill stem:

Table 2 shows that the results of boron reinforced epoxy fiber glass stem are very comparable with those obtained with titanium. However the

REPORT OF TESTS
TO MEASURE THE RISE OF BIT TEMPERATURES
DURING THE DRILLING OF DENSE BASALT

by

Marcus G. Langseth, Jr. and Richard Perry

Purpose:

The purpose of these tests is to determine the temperature rise in the vicinity of the drill bit during the drilling of solid basalt.

Equipment:

A. Drilling:

- 1. Black and Decker rotary percussive power head.
- 2. Two sections of boron reinforced drill stem.
- 3. Two sections of fiber glass drill stem reinforced with axially aligned glass fibers.
- 4. One solid-faced 1.027" diameter drill bit.
- 5. One coring bit (badly damaged) 1.027" in diameter.
- 6. One block of dense basalt.

B. Temperature measurement:

- 1. Three copper-construction thermocouples.
- 2. One ice bath.
- 3. One terminal board and rotary switch.
- 4. Ice bath for reference junctions.
- 5. Insulated thermocouple mounting board.

Description:

See Figure 1. The three thermojunctions were mounted in a piece of paperboard that is attached by a tape hinge to a second board. One of the

VARIAN RECORDER

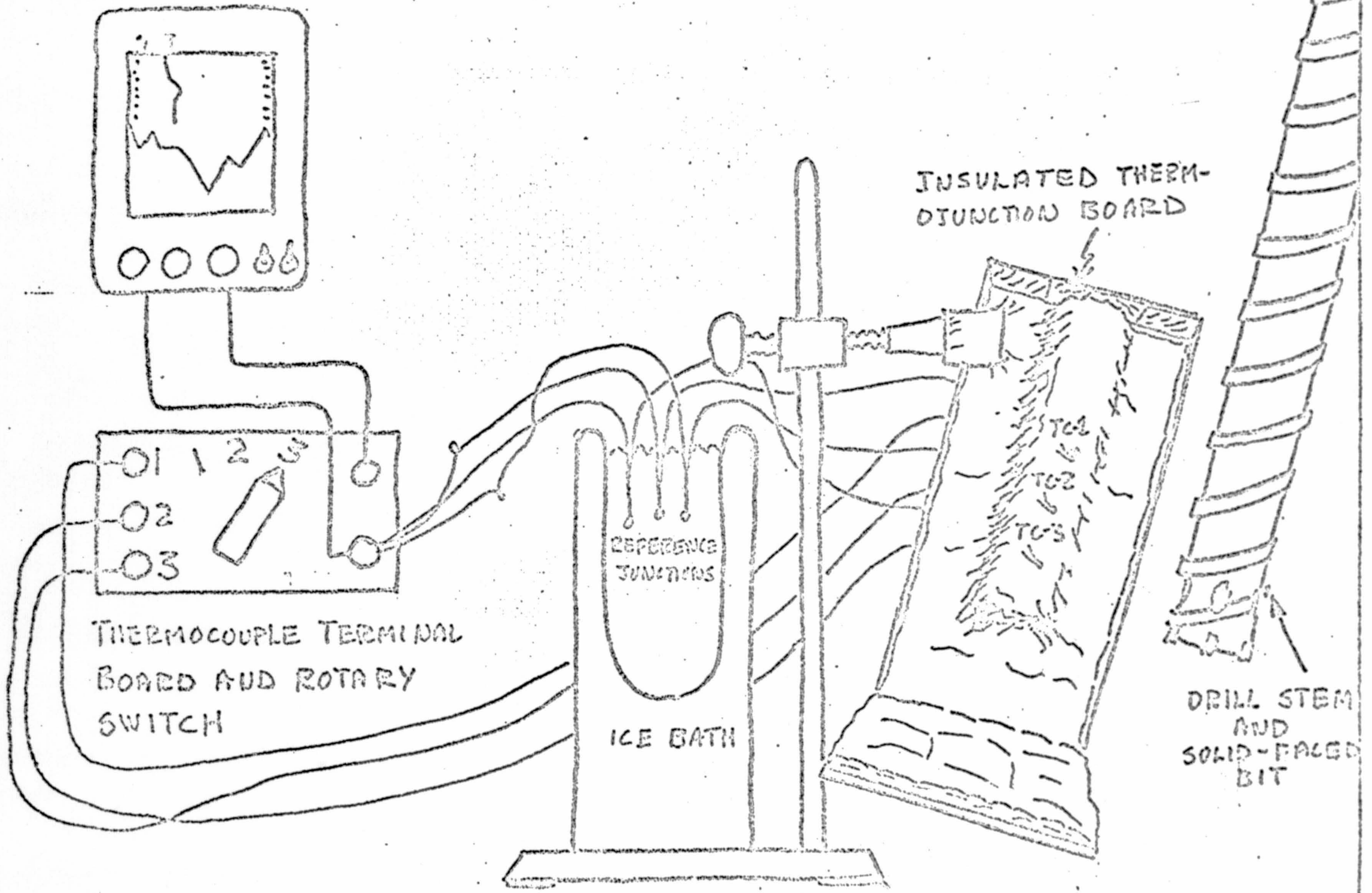


FIG 1 - SET UP TO MEASURE DRILL BIT TEMPERATURES

boards had an indentation to receive the end of the drill stem. The inside of the boards were covered by a thick soft 1/4" thick paper insulation. The thermocouples were mounted in such a way that when the drill stem was in the indentation and the boards closed together, the junctions made contact with the drill stem 1", 2", and 3" from the end of the drill stem. The junctions were coated with a heat sink compound.

The terminal board and rotary switch allowed the thermocouples to be switched one at a time into the Varian recorder. Full scale on the recorder equals about 200° C.

Procedure:

Using the B & D power head and the boron tube the hard basalt was drilled for a given duration of time (1 to 4 minutes). After completion of the drilling period, the lower end of the bit was transferred to and enclosed in the thermojunction board. Ten second readings of each thermocouple were made for about one minute.

Experiment results:

Table 1 shows the maximum temperatures reached by the three thermocouples.

TABLE I

| Run Number. | Duration of Drilling in Minutes | Temperature °C at thermocouple locations relative to bottom of the drill bit. | | |
|-------------|---------------------------------|---|----|------|
| | | 1" | 2" | 3" |
| 1 | 1 | 49 | 47 | 32 |
| 2 | 1 | 54 | 45 | 45 ? |
| 3 | 2 | 66 | 61 | 38 |
| 4 | 4 | 88 | 79 | 54 |
| 5* | 2 | 68 | 57 | 31 |

*Coring bit used on this run.

These results are plotted graphically in Figure 2.

Uncertainties and errors:

Nearly all errors will result in underestimation of true temperature.

The most important causes of error are:

1. Heat loss during the transfer of the drill from the hole to the thermocouple board. On the average this transfer can be made in about 5 seconds. Some earlier tests gave information about how rapidly the drill stem end and solid-faced bit cool in dry air as a function of temperature.

TABLE II

| Cooling rate of drill in still air as a function of temperature | |
|---|-----------------------------|
| Initial Temperature °C | $\Delta T/\Delta t$ °C/sec. |
| 176° C | 0.233 |
| 148° C | 0.200 |
| 120° C | 0.150 |
| 65° C | 0.100 |

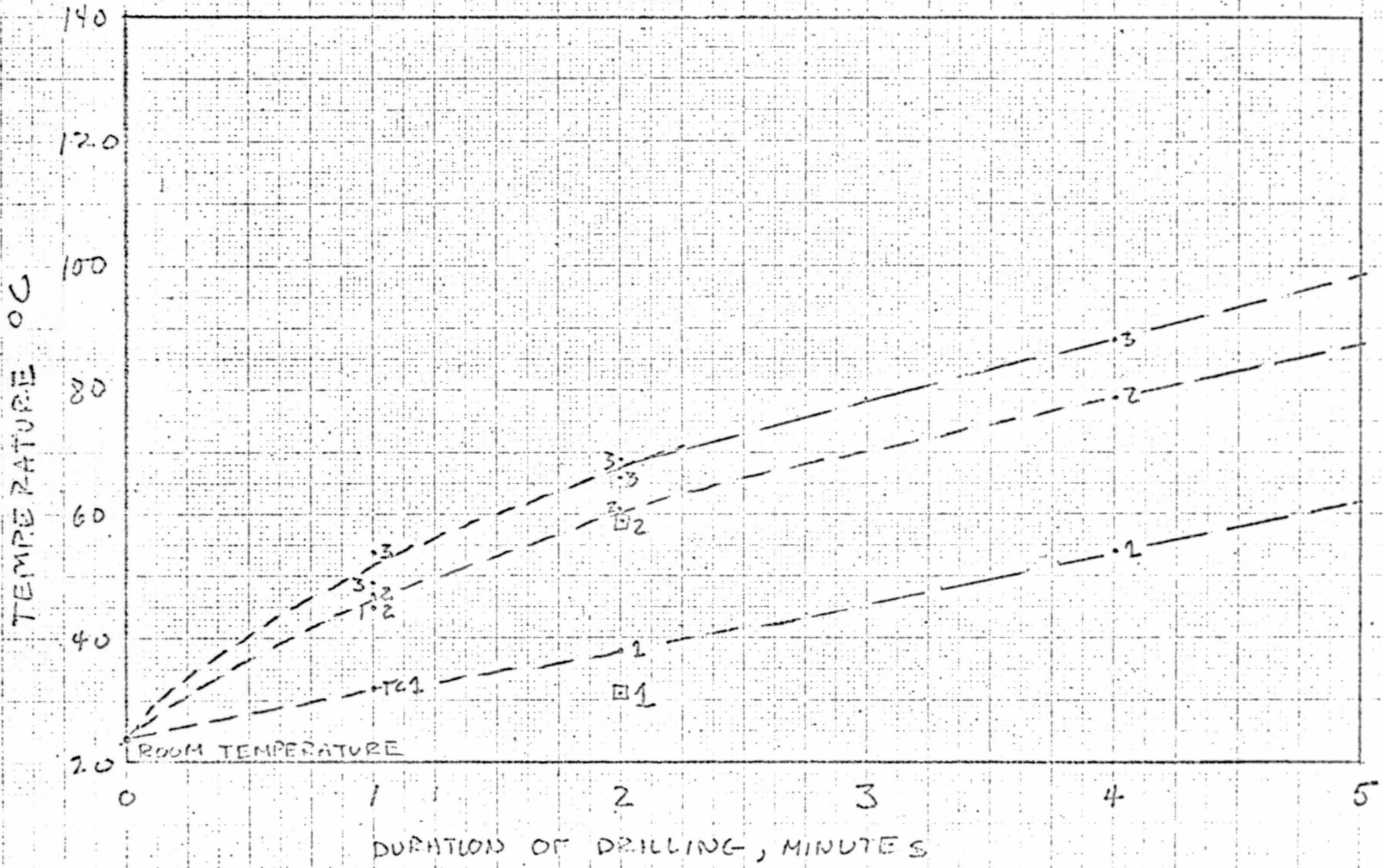


FIG. 2 TEMPERATURE RISE VERSUS TIME

From the results in Table II it is seen that the temperature drop during the transfer was probably from 1 to 2° C.

2. Poor contact between the drill stem and the thermocouples:

A strong effort was made to assure good contact. The thermocouple beads projected approximately 1/4" from the insulation so that when the drill stem was inserted, they would be spring loaded against it. Secondly, a silicon heat sink compound was dabbed on each thermocouple to decrease the contact resistance.

Good contact during a test run could be determined in two ways. a) The temperature trace obtained was steady; and b) The silicon heat-sink compound left a good smear on the drill stem. When operating properly, errors introduced in this way are probably less than -2° C.

The error of temperature measurement with the thermocouples based on tests in ice water and boiling water are no more than ±2° C.

Thus we conclude that at most the temperatures determined for the drill bit are underestimated by no more than 5° C.

Discussion:

Drill bit temperature during drilling:

Thermojunction #3 is placed so that it measures the temperature at the steel insert that holds the central carbide blade. The temperature rise at this location is seen to be roughly proportional to drilling time after an initial rapid rise. After three minutes the rate of rise of temperature is approximately 10° C per minute and after five minutes would reach about 105° C when errors are accounted for.

Thermojunction #2 is located so that it measures the temperature at the threaded joint between the drill bit and the stem. In the solid-faced bit this point is very well coupled thermally to the steel insert. Thus the temperatures at this point follow those of thermojunction #3 very well and appears it would reach a maximum of 95° C after five minutes of drilling in dense basalt.

Thermojunction #1 is placed to measure the temperature of the titanium drill stem one inch above the threaded coupling. The temperature at this point appears to rise much less rapidly and would reach a maximum of 70° C after five minutes of drilling.

One test using a coring bit was run for two minutes. The temperatures measured are shown as squares in Figure 2. Except for thermojunction #1 the results are very nearly the same as with the solid-faced bit. This result was unexpected since it was anticipated that large thermal mass of the solid-faced bit would result in substantially lower temperature. However, it appears that this effect is offset by the lesser amount of work done and the heat absorbed by the remaining internal rock core.

Additional considerations:

Although the cutting of rock in the drilling is the most important source of heat, a large amount of heat is also produced at joints due to mechanical mismatches particularly mismatches in elastic properties. Thus at joints where the fiber glass tube or stem is bonded to a metal insert, a great deal of stress working occurs and significant temperature rises result. Above certain temperatures this process becomes "run away" since the epoxy fiber glass begins to lose its elastic modulus and increased

working and heating results. This process resulted in failure at two bonded joints during the testing described here. In both cases, the bond broke down due to high temperatures. The bonding material loses its strength at temperatures greater than 70°C .

Several steps can be taken to minimize the above dangers.

1. Remove any bonded joint at least 2 inches from the coupling with the drill bit to avoid temperature rise from heat conducted up from bit face.

2. At each joint try to avoid mechanical mismatches to whatever extent possible by matching elastic properties and mass per unit length closely across the joint. This may be a major problem of designing the adapter.

3. Use epoxy compounds and bonding agents that retain their strength at temperatures up to 150°C at all joints.

4. Use circumferential wraps to radially strengthen bonded joints.

Recommendation: The body of the adapter being built for the boron filament drill stem should have the following dimensions.

